Learning and Managing Stochastic Network Traffic Dynamics with an Aggregate Traffic Representation

Wei Liu[a,b,c], Wai Yuen Szeto[d,*]

[a] *School of Computer Science and Engineering, University of New South Wales, Sydney, NSW 2052, Australia*

[b] *Research Centre for Integrated Transport Innovation, School of Civil and Environmental Engineering, University of New South Wales, Sydney, NSW 2052, Australia*

[c] *School of Engineering, University of Glasgow, Glasgow G12 8QQ, United Kingdom*

[d] *Department of Civil Engineering, The University of Hong Kong, Pokfulam Road, Hong Kong*

Abstract

This study estimates and manages the stochastic traffic dynamics in a bi-modal transportation system, and gives hints on how increasing data availability in transport and cities can be utilized to estimate transport supply functions and manage transport demand simultaneously. In the bi-modal system, travelers' mode choices are based on their perceptions of the two travel modes: driving or public transit. Some travelers who have access to real-time road (car) traffic information may shift their mode based on the information received (note that real-time information about public transit departures/arrivals is not considered here). For the roadway network, the within-day traffic evolution is modeled through a Macroscopic Fundamental Diagram (MFD), where the flow dynamics exhibits a certain level of uncertainty. A non-parametric approach is proposed to estimate the MFD. To improve traffic efficiency, we develop an adaptive pricing mechanism coupled with the learned MFD. The adaptive pricing extends the study of Liu and Geroliminis (2017) to the time-dependent case, which can better accommodate temporal demand variations and achieve higher efficiency. Numerical studies are conducted on a one-region theoretical city network to illustrate the dynamic evolution of traffic, the MFD learning framework, and the efficiency of the adaptive pricing mechanism.

Keywords: Traffic dynamics; stochastic MFD; information provision; learning; pricing.

*Corresponding author: ceszeto@hku.hk (W.Y. Szeto)

1 Introduction

The traffic equilibrium approach to planning and operation issues has been adopted for decades since it was firstly proposed by Wardrop (1952). To account for the time-varying traffic conditions and congestion dynamics, many efforts have been dedicated to the dynamic traffic assignment problem (Friesz et al., 1993; Lo and Szeto, 2002; Yildirimoglu and Geroliminis, 2014; Long et al., 2015). In particular, the within-day dynamic traffic patterns are governed by travelers' trip-timing choices, which have been modeled with the bottleneck model firstly proposed by Vickrey (1969). The bottleneck model has been extended by many studies (Arnott et al., 1990; Lindsey, 2004; Yang et al., 2013; Zhang et al., 2017; Liu, 2018) due to its analytical tractability to study a number of policy issues such as congestion pricing, user heterogeneity, commuter parking, shared-rides, and autonomous vehicles.

Other than within-day dynamics, traffic can vary from day to day. The day-to-day traffic dynamics can refer to the system traffic variations that occur between successive reference periods, as pointed out by the study of Cascetta and Cantarella (1991). A series of studies have modeled the day-to-day traffic evolution process for both single-mode systems (Smith, 1984; Watling, 1999; Bie and Lo, 2010; Cantarella, 2013; Smith and Watling, 2016; Guo and Huang, 2016) and multi-modal systems (Cantarella et al., 2015; Li and Yang, 2016; Liu and Geroliminis, 2017; Guo and Szeto, 2018). Some researchers have developed a doubly dynamical system (Ben-Akiva et al., 1984; Iryo, 2008; Liu et al., 2017; Guo et al., 2018; Yildirimoglu and Ramezani, 2019), which can describe the day-to-day evolution of within-day dynamic traffic patterns. However, existing studies along this direction, while insightful, often rely on simplified network or demand settings or traffic flow models (e.g., single origin-destination pair, single-mode systems, and point-queue traffic models).

Recently, there is a growing interest in modeling the impacts of information provision on traffic patterns. This is partly due to the rapid development of information technologies and devices (e.g., smart-phone, wearable devices, and connected vehicles), and the widespread use of smart navigation services and social media platforms. These emerging services and platforms now provide new opportunities for travelers to access traffic information and predicted conditions. Moreover, they can affect travelers' behaviors and decisions significantly, which further complicate the evolution of traffic and user choices in an integrated multi-modal transportation system. Analyzing the impacts of information provision/sharing becomes both necessary and relevant. However, little has been explored for day-to-day traffic evolution under real-time information provision, especially when the within-day traffic dynamics are very complex. Recent efforts towards these directions are made by e.g., Xiao and Lo (2016) for information sharing among travelers, and by e.g., Liu and Geroliminis (2017) for

real-time information provision through advanced smart services. A series of studies have explored the impacts of traffic information with static traffic models (Iryo, 2016; Bifulco et al., 2016; Li et al., 2018), while some studies are based on traffic simulators when examining the impacts of information provision (Mahmassani and Liu, 1999; Liu et al., 2017).

This study explores a stochastic dynamical process for the bi-modal transportation system and examines how the provision of real-time car traffic information can affect travelers' mode choices and the stochastic system traffic dynamics. Particularly, two types of users are considered, i.e., travelers using "smart services" and travelers not using any "smart services". Those using "smart services" have access to real-time road traffic information and their travel choices are affected by the real-time information. Therefore, both their past experiences and real-time information provision affect their choices, which is similar to the study of Liu and Geroliminis (2017). Those not using these services do not have access to or are not affected by real-time information. Different from the study of Liu and Geroliminis (2017) that assumed all users to have access to and be affected by information services, the treatment of multiple types of users in this study is more general.[1] In this paper, we focus on the impacts of real-time car traffic information, while the real-time information about public transit departures/arrivals is not considered. This means that the public transit service is the same for both types of travelers. Since information provision does not involve the public transit side, it does not save travelers' waiting time at transit stops.

The within-day traffic dynamics are modeled through the concept of Macroscopic Fundamental Diagram (MFD), which is supported by empirical evidence (Geroliminis and Daganzo, 2008). The MFD framework can capture hyper-congestion (Gonzales, 2015; Arnott et al., 2016; Lehe, 2017). Many studies based on the MFD concept assumed that the network outflow has an explicit relationship with the travel production and the trip length (Ramezani et al., 2015; Geroliminis, 2015; Liu and Geroliminis, 2016; Saeedmanesh and Geroliminis, 2016). Differently, this study only assumes a network/region speed function (speed-accumulation relationship). Similar to the studies of Arnott (2013), Fosgerau (2015), Leclercq et al. (2017), Mariotte et al. (2017), and Lamotte and Geroliminis (2018), this study uses a trip-based approach to reproduce the travel process of car traffic on roads. A discrete-time approximation for the trip-based approach was adopted in the numerical studies. Moreover, this study considers that the regional speed-accumulation relationship is subject to certain levels of random variations. The variability of the MFD relationship has been reported by many studies (e.g., Mazloumian et al., 2010; Daganzo et al., 2011; Gayah

[1] Firstly, the process of reaching 100% penetration for smart services can take a long time, even though it might be reached in the future. Secondly, the population is generally heterogeneous. While information services are growing rapidly, they may appear different in their accessibility, reliability etc. to different travelers (e.g., different age groups and education backgrounds).

and Daganzo, 2011; Geroliminis and Sun, 2011; Saberi and Mahmassani, 2012; Leclercq and Geroliminis, 2013; Gayah et al., 2014; Dakic and Menendez, 2018; Ambühl et al., 2018). Note that the stochasticity in the speed-accumulation relationship should not be extremely large. Otherwise, the MFD-based approach may be inappropriate since the regional speed-accumulation relationship may not exist in this case (when it is too random). For a recent review of MFD models, one may refer to Aghamohammadi and Laval (2018).

Beyond the developed day-to-day evolution model with stochastic traffic dynamics, we propose a data-driven and non-parametric approach to estimate the stochastic MFD (i.e., the speed-accumulation relationship in the paper) for the city road network. The proposed approach uses widely adopted smoothing strategies to translate the discrete data observations regarding traffic accumulation and the corresponding speed into numerical curves or approximations for the speed-accumulation relationship. It does not need prior knowledge regarding the functional form for the speed-accumulation relationship. This means that the approach is relatively general and can be adapted to cases with different speed-accumulation functions. To illustrate this, numerical tests for different speed functions were conducted. Based on the learned MFD, we develop a similar adaptive pricing strategy as that in the study of Liu and Geroliminis (2017) while we further extend it to the time-dependent case. Moreover, different from their study, a deterministic equilibrium flow pattern does not exist in the stochastic dynamical system modeled here, and thus the adaptive pricing strategy can no longer rely on stationary traffic conditions in a single day. Instead, the pricing strategy relies on average traffic conditions for a certain number of days to alleviate the random effects.

This study expands the literature on modeling and managing doubly dynamical systems in several ways. Firstly, this study integrates network-level stochastic within-day traffic dynamics into the day-to-day evolution modeling framework, which is very challenging and has rarely been explored in the literature. Secondly, time-dependent traffic conditions are incorporated into travelers' decision process, where we further extend the study of Liu and Geroliminis (2017) to a general case by considering two types of travelers, i.e., those with and without smart information services. Thirdly, we propose a non-parametric estimation approach for the regional MFD, which can take advantage of system traffic observations. This estimation approach is integrated with the day-to-day evolution modeling framework, which is novel compared to the literature. Fourthly, the learning mechanism for the MFD is further integrated with an adaptive pricing strategy, where we extend the time-independent pricing of Liu and Geroliminis (2017) to the time-dependent pricing case. This helps to accommodate time-varying demand conditions and further enhances system efficiency. Overall, this paper, by proposing a combined MFD learning/estimation and pricing adjustment framework, gives

hints on how increasing data availability in transport and cities can be utilized to estimate transport supply functions and manage transport demand simultaneously.

The remainder of the paper is organized as follows. Section 2 describes the basics of the bi-modal commuting problem, and introduces the regional speed-accumulation relationship with uncertainties. In Section 3, the day-to-day learning behaviors of travelers and the traffic adjustment process, the learning/estimation process of the MFD, and the adaptive pricing mechanism based on the estimated MFD are presented and discussed. Section 4 reports the numerical illustrations of the proposed models and mechanisms. Finally, Section 5 concludes the paper.

2 Basic Considerations

We now present the basic considerations for the rush-hour commuting problem with two modes to serve the travel demand. We consider the city of one region in Figure 1, where there are a roadway network system and a public transit system with a dedicated right-of-way.[2] Each location in the city/region can be indexed by its x-coordinate and y-coordinate, i.e., (x, y), and can be an origin and/or a destination. Let w be the origin-destination (O-D) pair and W be the set of all O-D pairs, and thus $w \in W$. Figure 1 is illustrative while there are indeed multiple origins and destinations. For each O-D pair w, travelers can either drive through the roadway network (private car: mode a) or take the public transit to reach their destinations (public transit: mode b). A list of major notations is provided in Appendix A.

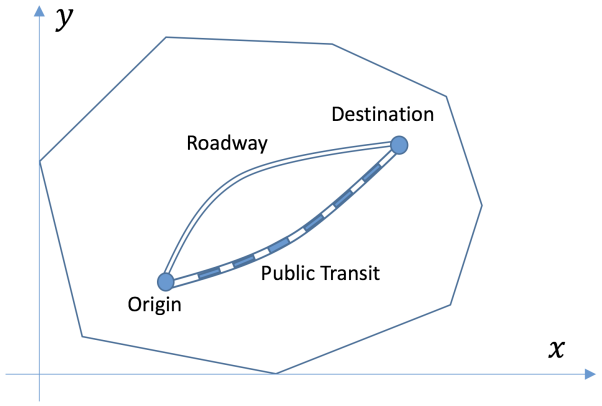

Figure 1: The city and transport system

[2]It is of our interest to extend the current model to the multiple-region case, where a network can be partitioned into multiple regions with a well-defined Macroscopic Fundamental Diagram (MFD) for each region by the approaches in the study of, e.g., Saeedmanesh and Geroliminis (2016). Multiple-region pricing strategies or controllers have to be adopted for improving traffic efficiency, such as those in the studies of, e.g., Ramezani et al. (2015), Kouvelas et al. (2017) and Haddad and Zheng (2018).

Now we move to the travel demand side. For a given departure time t and a given O-D pair w, the total travel demand $r^w(t)$ is assumed to be fixed and given. Thus, it does not change from day to day. Furthermore, we consider that there are two types of travelers among the demand: the first type (type s to refer to those with "smart services") has access to real-time car traffic information and is affected by the real-time information when making decisions, and the second type (type u to refer to those not using or not complying to "smart services") does not have access to or is not affected by the real-time information. Suppose the proportion of type s travelers is $\theta_s = \theta$, where $0 \leq \theta \leq 1$, and the proportion for type u is then $\theta_u = 1 - \theta$. Therefore, we have $r_s^w(t) = \theta_s \cdot r^w(t) = \theta \cdot r^w(t)$ and $r_u^w(t) = \theta_u \cdot r^w(t) = (1-\theta) \cdot r^w(t)$. While we will present the results of sensitivity analysis and examine the impact of different values for θ in the later part of this paper, we do not consider the endogenous evolution of θ in this paper. Moreover, we consider an identical θ value for travelers between each O-D pair and with each departure time (however, this can be easily relaxed with the current modeling framework). We denote those among type $k \in \{s, u\}$ choosing mode $m \in \{a, b\}$ by $r_{k,m}^w(t)$, where $r_{k,a}^w(t) + r_{k,b}^w(t) = r_k^w(t)$. The modeling duration is $[0, \Delta]$, and thus $t \in [0, \Delta]$.

Based on the above, the set of the feasible flows for private car and public transit modes for different types of travelers can be given as follows:

$$\Omega \equiv \left\{ r_{k,m}^w(t) \geq 0, \forall k, m, w, t \,\middle|\, \sum_m r_{k,m}^w(t) = r_k^w(t), r_k^w(t) = \theta_k \cdot r^w(t) \right\}. \tag{1}$$

It is evident that the feasible flow set Ω is closed and convex. Note that the realized traffic flow $r_{k,m}^w(t)$ on each day can be different. This will be discussed in Section 3 when we present the day-to-day evolution process.

2.1 Road Traffic Dynamics

We now describe the road traffic flow model for the private car mode. For the roadway network in the region (we consider a single region city), instead of modeling a detailed node-link network, we adopt an aggregate approach based on the recently proposed Macroscopic Fundamental Diagram (MFD), see the paper by, e.g., Geroliminis and Daganzo (2008). Particularly, the regional speed has a relationship with the regional traffic accumulation as follows:

$$v_a = v(n), \tag{2}$$

where v_a is the regional space-mean speed, n is the regional traffic accumulation, and $v(\cdot)$ is the speed function. The MFD framework defines region-based relationships among speed, traffic density/accumulation, and traffic flow. Alternatively, we can assume that the speed has a relationship with the regional traffic density. However, given the same roadway network setting and total road length, we can simply adopt the speed-accumulation relationship $v-n$, where network characteristics (e.g., the total road length, the road network topology, and the systematic signal setting) are input parameters. Since we adopt an aggregate traffic flow approach without detailed network setting, later we frequently use 'region' to refer to the roadway system or network.

A regional speed-accumulation relationship in Eq. (2) requires that the region modeled has a well-defined MFD with relatively low dispersion. In this paper, we assume a well-defined MFD for the region but with certain levels of variations or uncertainties (for the variability or uncertainty of an MFD, see the papers by, e.g., Geroliminis and Daganzo, 2008; Mazloumian et al., 2010; Daganzo et al., 2011; Gayah and Daganzo, 2011; Geroliminis and Sun, 2011; Saberi and Mahmassani, 2012; Leclercq and Geroliminis, 2013; Gayah et al., 2014; Dakic and Menendez, 2018; Ambühl et al., 2018). Generally speaking, a deterministic $v-n$ curve may not always be appropriate. Indeed, the MFD can be affected by changes in the road network itself or systematic signal plan changes or changes in management strategies. Moreover, the data observations to estimate an MFD may contain some random noises.[3]

In this study, we adopted the following functional form for the speed-accumulation relationship in the numerical analysis in Section 4:

$$v\left(n\right) \equiv \begin{cases} v_{cri} \cdot e^{\left(1-\frac{n}{n_{cri}}\right)} & \text{if } n \geq n_{cri}, \\ v_{cri} & \text{if } n < n_{cri}, \end{cases} \tag{3}$$

where v_{cri} and n_{cri} are the critical (maximum) speed and the critical accumulation, respectively. Beyond the critical accumulation, the speed (as well as travel production) starts to decrease with accumulation. To capture the stochasticity in the MFD-based traffic dynamics, we assume that v_{cri} and n_{cri} are both random variables.

We would like to highlight here that the above speed function in Eq. (3) is for reproducing traffic patterns in the modeled region. Different cities and regions may have different

[3]This raises our interest to develop a framework that can estimate the stochastic MFD of the network. Moreover, based on the MFD estimation that is updated over time, we can develop coupled adaptive management strategies to improve system traffic efficiency. An important advantage of doing so is that the management of the network system relies little on prior knowledge regarding the network, and can be adaptive and robust to system changes or variations.

functional forms for the speed-accumulation relationship. It has to be learned/estimated based on available data and the proposed learning/estimation mechanism. We will introduce a non-parametric estimation approach in Section 3.3 without requiring prior knowledge of the functional form for the regional speed-accumulation relationship. It is worth mentioning that different speed-accumulation functions can be readily accommodated in this paper (some numerical tests are presented in Appendix B3 for a different speed function than Eq. (3)). We adopt the current form because of three reasons. Firstly, it has been widely adopted in the literature. Secondly, it reflects the cases where speed remains approximately constant when there is no congestion (e.g., the speed may be subject to the speed limit in the city road network). Thirdly, it brings an important advantage that the speed is always non-negative, given that v_{cri} and n_{cri} are non-negative random variables.

2.2 Public Transit

For the public transit system, we assume that there are services with a dedicated right-of-way to serve each O-D pair w. Therefore, there is no direct interaction between car traffic and public transit vehicles. If the flow interaction between cars and transit vehicles was to be incorporated, similar frameworks such as the 3D-MFD in the studies of e.g., Geroliminis et al. (2014), Chiabaut (2015), and Loder et al. (2017) could be adopted. The new challenges associated with the 3D-MFD include, e.g., how to appropriately model a stochastic 3D-MFD, and how to estimate such a 3D-MFD. While the direct flow interaction between the two modes is not considered, the travelers' mode choices can affect traffic conditions, and in return affect other travelers' mode choices.

The transit service frequency is f_b^w, the transit fare is p_b^w, and the transit speed is v_b. Note that v_b is the average/commercial speed after taking into account pick-up and drop-off delays, intersection delays, and so on. Moreover, v_b is assumed to be constant (flow-independent). f_b^w and p_b^w are also assumed to be constant over clock time. However, time-dependent transit frequencies and/or fares are straightforward to be incorporated. Moreover, the transit service frequency and fare are fixed (do not change from day to day), while a future study may consider responsive services over (calendar) time (Zhang et al., 2014, 2016; Li and Yang, 2016; Zhang et al., 2018). These simplifications for transit services allow us to focus on the stochasticity and dynamics for the private car mode in the context of a doubly dynamical system.

3 Day-to-day Traffic Dynamics, Learning the Stochastic MFD, and Adaptive Pricing

Section 2 presents the background information regarding the travel demand and the two transport modes to serve the demand. Different from conventional bi-modal traffic equilibrium studies, this study, as mentioned in Section 1, models the day-to-day traffic evolution under stochastic MFD-based traffic dynamics and adjusts the congestion pricing levels adaptively from period to period. Therefore, we have to consider three time-scales. Firstly, we consider that the calendar time is divided into multiple periods and each period contains a number of days (and the clock time is considered in each day). At the beginning of each period, the road manager or operator may adjust the congestion pricing levels (period-to-period scale). Note that the MFD relationship for the region concerned has to be re-estimated in each period for adjusting the pricing levels. Secondly, given the updated pricing levels at the beginning of a period, we consider that the travelers may adapt their travel choices from day to day (day-to-day scale). Thirdly, for a given day, we model the interactions between commuters' travel choices and the (clock) time-varying traffic conditions (within-day scale). To alleviate the notation burden, we may either omit or include the indexes for (clock) times, days, and periods in different occasions.

In Section 3.1, we model the day-to-day evolution of commuters' travel choices under traffic information provision. This involves both the day-to-day and within-day scales. In Section 3.2, we present a detailed formulation for travel costs resulting from the within-day MFD dynamics. This mainly involves the within-day scale. In Section 3.3, we present the methodologies to learn from the traffic observations to provide an estimate for the MFD (of the studied region) that exhibits uncertainty, and develop methodologies to take advantage of the updated MFD estimation and observable traffic conditions to adjust the pricing levels. This mainly involves the period-to-period scale, and also involves the within-day scale when calculating the price adjustment based on the within-day road traffic conditions. For capturing the "big picture" of the overall modeling framework, readers may refer to Figure 4 at the end of Section 3.3.

3.1 Day-to-day Evolution Model

We consider a discrete-time day-to-day evolution model where the calendar day is denoted by q. For given O-D pair w and departure time t, the mean perceived travel cost on day q for mode m is denoted by $c_{k,m}^{p,w}(t,q)$. Similarly, the experienced cost is $c_m^{e,w}(t,q)$, and the predicted cost based on real-time information is $c_m^{r,w}(t,q)$ ("real-time instantaneous cost

estimate" hereafter). Note that here p, e, and r refer to perceived, experienced, and predicted costs, respectively. There is no k ($=s$ or u) index for the experienced cost and predicted cost, since the experienced costs are the same for both types of travelers as discussed in the following, and the predicted costs are not available to type u travelers.

For type s travelers who have access to real-time traffic information, the mean perceived travel cost of departing at time t on day $q+1$ is updated as follows:

$$c_{s,a}^{p,w}(t,q+1) = \eta_p \cdot c_{s,a}^{p,w}(t,q) + \eta_e \cdot c_a^{e,w}(t,q) + \eta_r \cdot (c_a^{r,w}(t,q+1) - c_a^{r,w}(t,q)), \tag{4}$$

where $\eta_p > 0$, $\eta_e > 0$, and $\eta_r > 0$ are three learning parameters associated with the previous perceived cost, experienced cost, and predicted cost, respectively, and $\eta_p + \eta_e = 1$. Eq. (4) means that the travelers' mean perceived cost on day $q+1$ is a linear combination of previous day's mean perceived cost and experienced cost, and plus the difference between the predicted costs for days $q+1$ and q. While the first and second terms in the right-hand side of Eq. (4) take travelers' past perceptions and experiences into account, respectively, the third term assumes that travelers compare the current traffic conditions with the ones he or she received from the previous day, and evaluate whether the situation today is worse or better. In particular, $c_a^{r,w}(t,q+1) - c_a^{r,w}(t,q) > 0$ indicates that the travel cost estimate based on the current traffic condition on day $q+1$ is larger than that on the previous day, which leads to an increase in the perceived cost since $\eta_r > 0$, and vice versa. A similar traveler learning model has been studied by Liu and Geroliminis (2017), which shows the potential for information to help the system traffic to converge to an equilibrium state or a fixed point, where the C-logit based stochastic user equilibrium was adopted by Liu and Geroliminis (2017). This is also verified in a recent study of Li et al. (2018) with static within-day traffic. Eq. (4) is a more general traveler learning model than that in, e.g., Bie and Lo (2010), where real-time traffic information has not been considered, i.e., $\eta_r = 0$.

Different from Liu and Geroliminis (2017), we further consider that there are type u travelers (the proportion in the whole population is θ_u). The mean perceived travel cost of departing at time t on day $q+1$ is updated as follows:

$$c_{u,a}^{p,w}(t,q+1) = \eta_p \cdot c_{u,a}^{p,w}(t,q) + \eta_e \cdot c_a^{e,w}(t,q), \tag{5}$$

where we still have $\eta_p > 0$, $\eta_e > 0$, and $\eta_p + \eta_e = 1$. Note that here we assume identical learning parameters $\eta_p > 0$, $\eta_e > 0$ for both types of travelers, which can be easily relaxed. Eq. (5) means that the type u travelers' perceived cost on day $q+1$ is a linear combination of day q's perceived cost and experienced cost. This is in line with existing learning models

(Watling, 1999; Bie and Lo, 2010) for travelers without real-time information. These travelers do not have access to or are not affected by real-time information/forecasts. Note that the perceived travel cost of travelers contain random terms, where $c_{k,a}^{p,w}$ in Eq. (4) or Eq. (5) is the mean value. The random terms of the perceived cost can be taken into account by using an appropriate discrete choice model (corresponding to the distributions of the random terms).[4]

For type k travelers (where $k \in \{s, u\}$), the proportion choosing mode m is based on

$$Pr_{k,m}^{w}(t, q+1) = \Phi_{k,m}^{w}\left(\mathbf{c}_{k}^{p}(t, q+1)\right), \tag{6}$$

where $Pr_{k,m}^{w}(t, q+1) \geq 0$ and $\sum_m Pr_{k,m}^{w}(t, q+1) = 1$. Note that $\Phi_{k,m}^{w}(\cdot)$ depends on the distribution of the random terms associated with the perceived travel cost. The expectation of flows on day $q+1$ at time t can be written as follows:

$$E\left(r_{k,m}^{w}(t, q+1) | \{\mathbf{r}(\tau, q), \tau \in [0, \Delta]; \mathbf{r}(\tau, q+1), \tau \in [0, t)\}\right) = r^{w}(t) \cdot Pr_{k,m}^{w}(t, q+1) \cdot \theta_k, \tag{7}$$

where $E(\cdot)$ denotes the expectation conditional on the realized traffic $\mathbf{r}(\tau, q)$ on day q and $\mathbf{r}(\tau, q+1)$ on day $q+1$ before time t. Eq. (7) simply says that the expected modal-split of travel demand at the current time is conditional on the realized traffic and demand conditions up to the current time point.

The above dynamical system defined by Eqs. (4)-(7) can be written in a vector-matrix form as follows:

$$\begin{Bmatrix} \mathbf{c}_{s}^{p}(t, q+1) \\ \mathbf{c}_{u}^{p}(t, q+1) \end{Bmatrix} = \eta_p \cdot \begin{Bmatrix} \mathbf{c}_{s}^{p}(t, q) \\ \mathbf{c}_{u}^{p}(t, q) \end{Bmatrix} + \eta_e \cdot \begin{Bmatrix} \mathbf{c}^{e}(t, q) \\ \mathbf{c}^{e}(t, q) \end{Bmatrix} + \eta_r \cdot \begin{Bmatrix} \mathbf{c}^{r}(t, q+1) - \mathbf{c}^{r}(t, q) \\ \mathbf{0} \end{Bmatrix}, \tag{8}$$

and

$$E\left(\mathbf{r}(t, q+1) | \{\mathbf{r}(\tau, q), \tau \in [0, \Delta]; \mathbf{r}(\tau, q+1), \tau \in [0, t)\}\right) = \begin{Bmatrix} \Phi_s(\mathbf{c}_{s}^{p}(t, q+1)) \cdot \mathbf{R}(t) \cdot \theta_s \\ \Phi_u(\mathbf{c}_{u}^{p}(t, q+1)) \cdot \mathbf{R}(t) \cdot \theta_u \end{Bmatrix}, \tag{9}$$

where $\mathbf{c}^{e}(t, q) = C^{e}(\mathbf{r}(\tau, q), \tau \in [0, \Delta])$, $\mathbf{c}^{r}(t, q) = C^{r}(\mathbf{r}(\tau, q), \tau \in [0, t))$, $\mathbf{c}^{r}(t, q+1) = C^{r}(\mathbf{r}(\tau, q+1), \tau \in [0, t))$, $\mathbf{R}(t)$ is a vector for total demand over different O-D pairs w at departure time t ($r^{w}(t)$ for different w). $C^{e}(\cdot)$ and $C^{r}(\cdot)$ are the cost functions, which are based on the physical characteristics of the roadway system and the transit systems (speed-

[4]To this point, we would like to summarize that there are two types of random terms in our modeling framework. The first type is related to the traffic flow model, i.e., the critical speed and accumulation, i.e., v_{cri} and n_{cri} given in Eq. (3). The second type is related to travelers' perceptions of travel costs, which results in the utilization of a certain discrete choice model.

flow relationship etc.), and the operations (toll charges, fares, frequencies etc.).

Note that the flow vector $\mathbf{r}(t, q+1)$ is a random vector that cannot be exactly predicted in advance. If we ignore the random fluctuations in demand or supply and suppose $\mathbf{r}(t, q+1) \equiv E\left(\{\mathbf{r}(\tau, q), \tau \in [0, \Delta]; \mathbf{r}(\tau, q+1), \tau \in [0, t)\}\right)$, Eq. (8) and Eq. (9) together becomes a deterministic process. For discussions regarding the fixed points of the deterministic dynamical system, one may refer to the study of Cantarella and Cascetta (1995).

This study focuses on the stochastic case, i.e., the dynamical system defined by Eq. (8) and Eq. (9). According to Cantarella and Cascetta (1995), if $\Phi_k(\cdot)$ where $k \in \{s, u\}$ is blockwise positive and continuous, and $C^e(\cdot)$ and $C^r(\cdot)$ are continuous, the resulting stochastic process is expected to be regular. As discussed by Cantarella and Cascetta (1995), $\mathbf{r}(t, q+1)$ in Eq. (9) can be determined through Monte-Carlo simulation based on the probability distributions of the stochastic process.

In this study, for simplicity, we adopted the following steps to replicate the traffic uncertainty and dynamics. Firstly, we adopted the binomial Logit-model for both type s and type u travelers for mode choices in the numerical experiments (i.e., the distribution of the perceived cost is known and identical every day). Specifically, we have

$$Pr_{k,m}^{w}(t, q+1) = \frac{e^{-\beta_m^w \cdot c_{k,m}^{p,w}(t, q+1)}}{\sum_{m'} e^{-\beta_{m'}^w \cdot c_{k,m'}^{p,w}(t, q+1)}}. \tag{10}$$

Note that the coefficient β_m^w is mode and O-D pair specific. For simplicity, in the numerical studies we adopted an identical value for all. The underlying assumption for the above Logit choice model is explained as follows. Let the random term associated with the perceived cost be ε_m^w , where $c_{k,m}^{p,w}$ is the mean perceived cost. The binomial logit model assumes that all ε_m^w are identically and independently distributed with a Gumbel probability distribution function, where the mean is zero and the variance is $\frac{1}{6}\pi^2\beta_m^w$. Empirically, the Logit-model above can reasonably reproduce the mode choice behavior if its parameters can be fitted with real observations. Secondly, the determination of the mean perceived travel cost $c_{k,a}^{p,w}(t, q+1)$ depends on the predicted cost, which is governed by the realization of roadway performance over time (e.g., the speed in this paper). In this paper, it is determined through a single-run Monte-Carlo simulation for speed at every time point on the day considered. This simulation indeed replicates the traffic process at an aggregate level (where the probability distributions of speed at different times are independent of each other).

3.2 Traffic Performance and Cost Components

Now we discuss how the experienced cost and real-time instantaneous cost estimates (which simulate the input of real-time information) can be determined for the bi-modal system.

Experienced conditions and costs. For all travelers between O-D pair w, suppose the trip distance is l_m^w for mode m. While the trip distance is O-D pair and mode specific, we consider that for different types of travelers and departure times, the trip distance is identical. Based on the regional speed-accumulation relationship, the experienced private car travel time (driving time) $T_a^w(t)$ can be determined by solving the following equation (the driving time is in the upper limit of the integral):

$$\int_t^{t+T_a^w(t)} v_a^e(\tau)\, d\tau = l_a^w, \tag{11}$$

where $v_a^e(\tau)$ is the realized speed at time τ for the region, and l_a^w is the driving distance, which is time-invariant. Eq. (11) says that for a traveler between O-D pair w who departs at time t, the distance traveled between time t and time $t+T_a^w$ is equal to his or her trip distance. This is a trip-based approach, which is similar to the studies of e.g., Fosgerau (2015), Lamotte and Geroliminis (2018), and Mariotte et al. (2017). Under such a trip-based concept, only a regional speed-accumulation relationship $v(n)$ is adopted, while arrivals to destinations are specific to individual trips based on Eq. (11). Specifically, at every time t' in the simulation, we check if $\int_t^{t'} v_a^e(\tau)\, d\tau = l_a^w$ numerically. If yes, it means that these travelers, i.e., $r_{k,a}^w(t)$, have arrived at their destination at time t', and should be counted as a part of the total outflow. Differently, in the study of Liu and Geroliminis (2017), an MFD-based outflow model is further assumed, i.e., the outflow or arrival rate to destination is proportional to the travel production $v(n) \cdot n$ and is inversely proportional to the trip distance, which is usually more accurate in steady state conditions.[5]

Following the above discussion, flows departing before time t arrive before time $t+T_a^w(t)$.

[5]There are at least two advantages of taking a trip-based approach in this study. Firstly, as discussed in Mariotte et al. (2017), the trip-based approach is generally more accurate than non-trip-based approaches (or accumulation-based approaches) when demand and congestion conditions change quickly over time. This means that the trip-based approach better fits the doubly dynamical modeling framework in this paper, which is to model traffic dynamics that can change quickly. Secondly, within the trip-based modeling framework, the experienced travel time of each trip is calculated as a byproduct (to check whether a trip is completed), which can then be directly utilized for updating travelers' choices on the following day (day-to-day evolution framework). However, it should be noted that when compared to the non-trip-based approach in the study of Liu and Geroliminis (2017) under a similar doubly dynamical system, the trip-based approach requires longer computation time since trips have to be tracked.

For traffic between O-D pair w, the cumulative outflow and inflow satisfy

$$O^w(t + T_a^w(t)) = \sum_k R_{k,a}^w(t), \tag{12}$$

where $O^w(t + T_a^w(t))$ is the cumulative outflow for O-D pair w at time $t + T_a^w(t)$ and $R_{k,a}^w(t)$ is the cumulative inflow at time t for type k drivers between O-D pair w. By taking the first-order derivative of Eq. (12) with respect to time t, we have

$$o^w(t + T_a^w(t)) = \frac{\sum_k r_{k,a}^w(t)}{1 + \frac{dT_a^w(t)}{dt}}, \tag{13}$$

where $o^w(t + T_a^w(t))$ is the outflow for O-D pair w at time $t + T_a^w(t)$ and $r_{k,a}^w(t)$ is the inflow at time t for type k drivers between O-D pair w. This is similar to that in the study of, e.g., Chow (2009) under a continuous-time model formulation. Together with traffic conservation, the accumulation in the network can be determined. Note that in this paper we focus on a single city region, and we consider that cars can always enter the network even if the road network is already very congested (inflows are not restricted) and there is also no rigid upper bound for the outflows (however, outflows are governed by the speed). Nevertheless, it is more realistic to include boundary capacities in the formulations, especially when we extend the current framework to multiple-regions (e.g., when one region is extremely congested, the inflows to that region should be restricted).

The above formulations and calculations in Eq. (11), Eq. (12) and Eq. (13) are based on a continuous-time modeling framework. In the numerical case, the (clock) time horizon is discretized into identical intervals (the length is denoted by δt), and then we need to use discrete-time approximations. We now briefly discuss the discrete-time approximation for travel time and outflow in this paper. For the travel time $T_a^w(t)$ in Eq. (11), we use a similar approach to that in the study of Liu and Geroliminis (2017) for estimating the experienced cost (one may refer to "Section 3.2" in their paper), which is summarized as follows. To avoid additional notation burdens, we still use t to indicate the time interval after the discretization of the time horizon. The travel time $T_a^w(t)$ (for departing in time interval t) can be determined as follows:

$$T_a^w(t) = (z_1 + z_2) \cdot \delta t, \tag{14}$$

where z_1 is a non-negative integer and z_2 is a non-integer (unless it is equal to zero), and

$0 \leq z_2 < 1$. The values of z_1 and z_2 can be determined by solving the following

$$l_a^w = \begin{cases} \sum_{\tau=t}^{t+z_1-1} \left[v_a^e(\tau) \cdot \delta t\right] + z_2 \cdot v_a^e(t+z_1) \cdot \delta t \text{ if } z_1 \geq 1, \\ z_2 \cdot v_a^e(t) \cdot \delta t \text{ if } z_1 = 0, \end{cases} \tag{15}$$

where $0 \leq z_2 < 1$ should always hold, and $\sum_{\tau=t}^{t+z_1-1} v_a^e(\tau) \cdot \delta t \leq l_a^w < \sum_{\tau=t}^{t+z_1} v_a^e(\tau) \cdot \delta t$ for $z_1 \geq 1$, and $l_a^w < v_a^e(t) \cdot \delta t$ for $z_1 = 0$. It can be verified that the first-in-first-out principle holds for the inflow between the same O-D pair and with the same trip length, i.e., $\sum_k r_{k,a}^w(t-1)$ arrives at the destination no later than $\sum_k r_{k,a}^w(t)$.

Given the travel time in Eq. (14) based on the discrete-time approximation, the outflow can be determined accordingly. The inflow in time interval t, i.e., $\sum_k r_{k,a}^w(t)$, which is counted in the cumulative inflow $\sum_k R_{k,a}^w(t)$ in time interval t, arrives at the destination in time interval $t + z_1$ since $z_1 \cdot \delta t \leq T_a^w(t) = (z_1 + z_2) \cdot \delta t < (z_1 + 1) \cdot \delta t$. Therefore, $\sum_k r_{k,a}^w(t)$ is a part of the cumulative outflow $O^w(t+z_1)$, and a part of the outflow $o^w(t+z_1)$ in time step $t + z_1$. This is a discrete-time approximation of the flow conservation in Eq. (12). However, it should be noted that $o^w(t + z_1)$ is not necessarily equal to $\sum_k r_{k,a}^w(t)$, i.e., $o^w(t + z_1) \neq \sum_k r_{k,a}^w(t)$ may hold. For example, for the inflow $\sum_k r_{k,a}^w(t-1)$ in time step $t - 1$, if the travel time $T_a^w(t-1)$ satisfies $(z_1 + 1) \cdot \delta t < T_a^w(t-1) < (z_1 + 2) \cdot \delta t$ (in this case $T_a^w(t-1) > T_a^w(t)$), the inflow $\sum_k r_{k,a}^w(t-1)$ in time step $t - 1$ is also a part of outflow in time step $t + z_1$ (i.e., $t - 1 + z_1 + 1$), and $o^w(t + z_1)$ includes both $\sum_k r_{k,a}^w(t-1)$ and $\sum_k r_{k,a}^w(t)$. This is indeed a reflection of the continuous-time outflow formulation in Eq. (13) in the discrete-time approximation (for $\frac{dT_a^w(t)}{dt} \neq 0$).

For both the travel time and outflow, our discrete-time approximation based on the discretization of the time horizon into multiple intervals can lead to inaccuracy because of the following. Firstly, within each small time interval after discretization, the accumulation is assumed constant and so is the speed. Secondly, arrivals occurring at different time points but within the same time interval are considered to be an outflow in the same time interval (outflow aggregation). One can expect that the results from our discrete-time approximation can be very inaccurate unless the length of the time interval δt is sufficiently small.

We now turn to the transit travel time. Based on the setting of the public transit system in Section 2, the transit travel time, which consists of both waiting time and in-vehicle time, can be written as

$$T_b^w(t) = \frac{1}{2f_b^w} + \frac{l_b^w}{v_b}, \tag{16}$$

where f_b^w is the service frequency, $\frac{1}{2f_b^w}$ is the average waiting time[6], l_b^w is the trip length of taking the transit, and v_b is the average speed of transit services. Note that here the transit cost is simplified where walking/access time, transfer time etc. have not been incorporated, and the values of waiting time and in-vehicles time are treated equally, while the extension to accommodate these issues would be straightforward, see the paper by, e.g., Amirgholy et al. (2017). Also, heterogeneous travelers such as those in the studies of Liu et al. (2014) and Amirgholy and Gonzales (2017) are not taken into account.

For travelers between O-D pair w and departing at time t, the experienced travel cost of mode m is the sum of travel time cost and monetary cost, which is given by

$$c_m^{e,w}(t) = \alpha \cdot T_m^w(t) + p_m^w(t), \tag{17}$$

where α is the value of time (VOT), $T_m^w(t)$ is the travel time of mode m, and $p_m^w(t)$ is the monetary cost.

The monetary cost $p_a^w(t)$ should generally include parking fees, congestion charges etc. In the current study, we let it be the congestion charge, which is a variable that can be optimized (parking fees etc. can be readily incorporated by adding a constant or variable price). It follows that $p_a^w(t)$ is the congestion charge for the travelers between O-D pair w entering the network at time t. $p_b^w(t)$ is simply the public transit fare, which in this study is considered time-invariant, i.e., $p_b^w(t) = p_b^w$.

Predicted conditions and costs. We now discuss the instantaneous cost estimate based on real-time traffic conditions. The instantaneous cost estimate for private cars can be determined in a similar way as the experienced cost. We need to replace the experienced speed $v_a^e(\tau)$ in Eq. (11) with the speed $v_a^e(t)$ at departure time t to have an instantaneous estimation of travel time. It then follows

$$c_a^{r,w}(t) = \alpha \cdot \left[\frac{l_a^w}{v_a^e(t)}\right] + p_a^w(t), \tag{18}$$

where $\frac{l_a^w}{v_a^e(t)}$ is the travel time estimate of private cars, and $p_a^w(t)$ is still the congestion charge.

While the above instantaneous speed based cost estimates are indeed studied and used in the literature and practice, these estimates are generally different from the experienced costs (as the speed can vary during the journey). Current smart information services already

[6]Note that the real-time information provision considered in this paper is about road (car) traffic conditions, but not public transit departure/arrival information. Therefore, for both types of travelers, the transit travel time includes a waiting time. If we consider that those travelers with information services know the exact public transit departure/arrival times, the waiting time is zero (or a small constant in practice), and we have $T_b^w(t) = \frac{l_b^w}{v_b}$ for these travelers.

provide the prediction that takes into account the variations in the traffic condition of the network within the duration of the individual trips (e.g., Herrera et al., 2010; Hofleitner et al., 2012). A vast literature in travel time estimations indicates that the discrepancy between the experienced time and the instantaneous estimation of travel time for smoothly varying traffic conditions may be in the range of 5-10%, see the paper by, e.g., Yildirimoglu and Geroliminis (2013). It is necessary and relevant to consider how different types of predictions may affect traveler choices and traffic dynamics differently. It is of our interest to combine historical data and real-time data or to utilize simulations to produce other types of predictions and compare them in our future study. Recent efforts along this line can be found in Liu et al. (2017) and Li et al. (2018). As pointed out by Bifulco et al. (2016) and Li et al. (2018), less accurate traffic predictions may result in larger variations in traffic patterns and a larger traffic instability. It was also pointed out by Li et al. (2018) that very inaccurate information provision could result in non-compliance with the predicted conditions. In this case, information provision becomes obsolete.

For the public transit, besides assuming a dedicated right-of-way, it is further assumed that the transit service has a constant (commercial) speed (over the clock time). We then have $c_b^{r,w}(t) = c_b^{e,w}(t)$. This treatment has simplified the dynamics and stochasticity in the public transit side, which allows us to focus on the dynamics and stochasticity for car traffic.[7]

3.3 Learning the Stochastic MFD and Adaptive Pricing

We now discuss in detail the learning/estimation mechanism for the stochastic MFD and the coupled adaptive pricing strategy.

Learning the MFD. After observing traffic conditions from day ONE to day q', the historical data regarding accumulation and speed can be determined. Let $n^e(t,q)$ and $v_a^e(t,q)$ be the realized accumulation and speed at time t on day q, respectively, for $q = 1, 2, ..., q'$. These become known and available after day q'. Note that in this paper, how to obtain $n^e(t,q)$ and $v_a^e(t,q)$ from traffic data is not discussed but it can be found in the study of Geroliminis and Daganzo (2008). The relationship between $v_a^e(t,q)$ and $n^e(t,q)$ can then be estimated accordingly. We adopt a data-driven and non-parametric estimation approach

[7]The dedicated right-of-way and constant speed assumptions for public transit indicate that the transit service is unchanging. Therefore, the effect of gaining real-time information about the schedule and operation of the transit mode becomes less relevant, as both travelers with and without real-time information know the service schedule (the experienced condition is the same as the predicted condition). Future study may incorporate stochasticity in the transit side. Obtaining real-time information may reduce waiting time for travelers at origin stops. In principle, these features could be easily accommodated within the current modeling framework. However, more types of inter-correlated impacts of information provision for both modes on the bi-modal system should be considered, which is challenging. We will more comprehensively explore this issue in the future.

without any prior assumption regarding the $v-n$ curve adopted in Section 2. That is, for the estimation process, we do not assume any functional form for the $v-n$ relationship, and we do not assume any distribution for the random variables involved. Doing so makes our approach more general such that it can be applied to different cases where the $v-n$ relationship may vary. As one may imagine, the data points $(v_a^e(t,q), n^e(t,q))$ are discrete points in the feasible domain, i.e., $(v_a^e(t,q), n^e(t,q)) \in H$. This suggests that some smoothing strategies are needed to estimate the curve for the $v-n$ relationship. We discuss this in the following.

The first and simplest way is to estimate $v(n)$ and $v(n)\cdot n$ through the local averages similar to the simple moving average method. We can define a critical gap value for accumulation, i.e., δn. If $n-\delta n \le n^e(t,q) \le n+\delta n$, we include the data point $(v_a^e(t,q), n^e(t,q))$ in the set H_n, i.e., $(v_a^e(t,q), n^e(t,q)) \in H_n \subset H$. Then we can calculate the mean values as follows:

$$E\left(v(n)\right) = \frac{\sum v_a^e}{|H_n|}; E\left(v(n)\cdot n\right) = \frac{\sum v_a^e \cdot n^e}{|H_n|}, \tag{19}$$

where $|H_n|$ is the size of H_n (the number of elements in the set H_n). Note that δn should be sufficiently large such that H_n is not an empty set. We can then determine the critical accumulation as follows:

$$n_{cri} \equiv \arg\max_n \{E\left(v(n)\cdot n\right)\}. \tag{20}$$

Accordingly, we can let $v_{cri} = E(v(n_{cri}))$.

The second way is through Nadaraya-Watson kernel regression (Nadaraya, 1964; Watson, 1964), which is to estimate $v(n)$ and $v(n)\cdot n$ as locally weighted averages using a kernel as the weighting function. Particularly, we use the Gaussian kernel, where the Gaussian Kernel Function is $K(\mu) = \frac{1}{\sqrt{2\pi}} \cdot \exp^{-\frac{1}{2}\cdot\mu^2}$. As the weighted average for $v(n)\cdot n$ can be determined, n_{cri} can be calculated similar to Eq. (20), and v_{cri} can be further determined accordingly. Note that we tested both ways (based on simple moving averages and Nadaraya-Watson kernel regression) in the numerical analysis, where we found that the estimation through the second way was smoother, and thus we used the Nadaraya-Watson kernel regression based approach for our MFD learning in the numerical examples.

It is worth mentioning that rather than estimating or approximating the $v-n$ curve based on all available data from day ONE to day q', it may be necessary to restrict the data set to only contain traffic observations within a certain number of days before day q'. This makes the learning mechanism "adaptive" or "dynamic". That is, we utilize relatively updated data to estimate the MFD; in case the MFD itself changes over (calendar) time due to network variations, the mechanism itself always provides an updated and accurate estimation. In the numerical studies, we utilized traffic observations for 15 days to estimate

the regional MFD, and a period also contains 15 days.

The procedure for estimating n_{cri} and v_{cri} through Nadaraya-Watson kernel regression is described in the following. However, to save space, we omit the estimation procedure based on the moving average method.

Algorithm Nadaraya-Watson kernel regression based MFD estimation

Establish $n_{min} = \min\{n^e\}$ and $n_{max} = \max\{n^e\}$ for $(v_a^e, n^e) \in H$

$h = 50$ ▷ bandwidth for the Gaussian kernel

$N = 1 \times 10^4$ ▷ number of steps for the interval $[n_{min}, n_{max}]$ and $\delta n = \frac{n_{max} - n_{min}}{N-1}$

$\boldsymbol{n} = linespace[n_{min}, n_{max}, N]$ ▷ $\boldsymbol{n} = [n_1, n_2, ..., n_N]$

for $i = 1 : N$ **do**

$$n_i \cdot v(n_i) = \frac{\sum_{n^e} K\left(\frac{n_i - n^e}{h}\right) \cdot n^e \cdot v_a^e}{\sum_{n^e} K\left(\frac{n_i - n^e}{h}\right)}$$ ▷ $K(\cdot)$ is the Gaussian Kernel Function

end

$i_{cri} = \text{argmax}_i \, n_i \cdot v(n_i)$

$n_{cri} = n_{i_{cri}}$ and $v_{cri} = v(n_{cri})$

Adaptive Pricing. Now we turn to discuss the adaptive pricing scheme, which takes advantage of the estimated MFD and observed system traffic conditions (system feedback). When reading through the proposed adaptive pricing strategy in the following, readers are suggested to keep in mind that under the MFD framework, later travelers can also create additional congestion for earlier travelers and travelers entering the network at different times can affect each other's experienced traffic conditions. This is because under the MFD framework, the regional speed depends on all traffic in the region. Three key aspects are specified in the following before we formulate the pricing adjustment scheme.

The stochastic MFD might be re-estimated from day to day once new observations become available, as discussed in the above. However, the pricing scheme should generally not change too frequently, mainly due to two reasons. Firstly, it takes time for travelers to stabilize their choices from a day-to-day point of view given a pricing scheme; secondly, system operators should not let travelers get frustrated by frequently changing prices. Therefore, the pricing scheme should only be adjusted from period to period, where a period contains a certain number of days, e.g., one month, and we can adjust the price at the beginning of each period. Let g be the period. For the ease of presentation, we add the period index g rather than the day index q to the prices. Thus, we have $p_m^w(t, g)$.

The second aspect is that, for a (departure) time t, the adjustment of pricing may rely on not only traffic conditions observed at time t but also the conditions relevant to this time point. This is explained as follows. Firstly, as t is the departure time and the pricing level is departure-based, the pricing level affects the number of users departing at time t and therefore the traffic conditions at time points following time t. This means that we may need

to consider traffic conditions after time t as system feedback for the pricing adjustment at time t. Secondly, if before time t, traffic conditions are already in a congested and inefficient state, we may also want to increase the price at time t to avoid further worsening congestion, and vice versa. This means that traffic conditions before time t may also be incorporated in the pricing adjustment. Indeed, for every t, we can define a time duration γ_t, where $t \in \gamma_t$, during which the observed conditions are considered in updating the pricing level at time t. To appropriately set the length of γ_t is an interesting direction for future research, but an initial estimate can be twice of the average travel time for users departing around time t (travelers departing at time points outside this time window have a marginal effect as most of them should have little interaction with travelers departing at time t in the network).

In addition to the above, there is another aspect to be considered, i.e., how many days of observed conditions should be taken into account so that we can have a good approximation of system performance under certain pricing schemes. This is necessary as the traffic dynamics and traveler choices are all stochastic. On one side, generally we expect that the traffic conditions on the days too far away from the current day are less relevant to the traffic condition on the current day, and therefore the number of days to consider should be upper-bounded. On the other side, it seems reasonable to include at least a number of days to alleviate the random effects of traffic conditions in a single day. Let us define a critical day gap as δq, and we consider conditions from day $\max\{1, q' - \delta q + 1\}$ to day q' to compute the estimate/expectation for conditions given the same pricing scheme. In this study, the value of δq is given, and the MFD learning and adaptive pricing framework does not involve the determination of δq. However, the sensitivity analysis regarding δq can be conducted to identify an appropriate δq. In the numerical studies, we used 5 days.

We now can present the congestion charge adjustment as follows:

$$\begin{aligned} p_a^w(t, g+1) = p_a^w(t, g) \\ +p_{a,0}^w \cdot \int_{\tau \in \gamma_t} \max\{0, n_{ave}^{e,g}(\tau) - n_{cri}^g\} d\tau \\ -p_{a,0}^w \cdot \int_{\tau \in \gamma_t} \max\{0, n_{cri}^g - \max_{\tau \in \gamma_t}\{n_{ave}^{e,g}(\tau)\}\} d\tau \end{aligned}, \tag{21}$$

where $p_a^w(t, g+1)$ is the pricing level at time t for period $g+1$ (next period); $p_a^w(t, g)$ is the pricing level for period g (current period); $p_{a,0}^w$ is the coefficient for pricing adjustment (which indeed translates delays into prices, as will be discussed shortly); n_{cri}^g is the estimated critical accumulation for period g; and $n_{ave}^{e,g}(\tau)$ is the average condition for period g that takes into account only a number of days at the end of the period (from day $\max\{1, q' - \delta q + 1\}$ to day q' as mentioned earlier). If we plot $n_{ave}^{e,g}(\tau)$ and n_{cri}^g in Figure 2, the second and third terms

in Eq. (21) can be well interpreted as follows.

We take the two time points t_1 and t_2 in Figure 2 as examples and firstly highlight the shadow areas' association with the terms in Eq. (21). For time t_1 and t_2, suppose both γ_{t_1} and γ_{t_2} are identified by the dotted-dashed lines. For the case of t_1, based on the average values over a few days, the considered duration is congested (at least for some duration within γ_{t_1}, $n^{e,g}_{ave}$ goes beyond the critical value). We then calculate the size of the shadow area, which is exactly the second term on the right-hand side of Eq. (21) without the coefficient $p^w_{a,0}$. This area is indeed the additional congestion delays due to the fact that the accumulation goes beyond the critical value. Note that in this case, the third term on the right-hand side of Eq. (21) is zero. Now let us move to the case of time t_2. As one can see, during the considered duration γ_{t_2} characterized by the two dotted-dashed lines, the average value $n^{e,g}_{ave}$ is always below the critical value. In this case, the second term on the right-hand side of Eq. (21) becomes zero, while the size of the corresponding shadow area is the total number of additional vehicles (aggregated over time) that can be allowed into the network without causing the maximum accumulation to go beyond the critical level. The area corresponds to the third term on the right-hand side of Eq. (21) but again without the coefficient $p^w_{a,0}$. It now becomes evident that the price in the new period is based on the last price (the first term on the right-hand side), the additional congestion delays (the second term on the right-hand side), and the wasted roadway capacity (the third term on the right-hand side). The procedure to determine the pricing adjustment is shown in the flowchart in Figure 3.

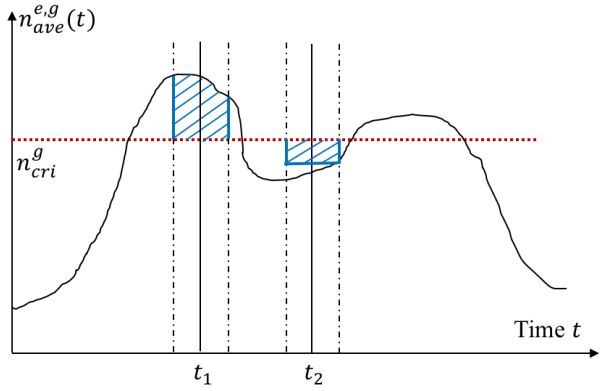

Figure 2: Graphical explanation of the pricing adjustment

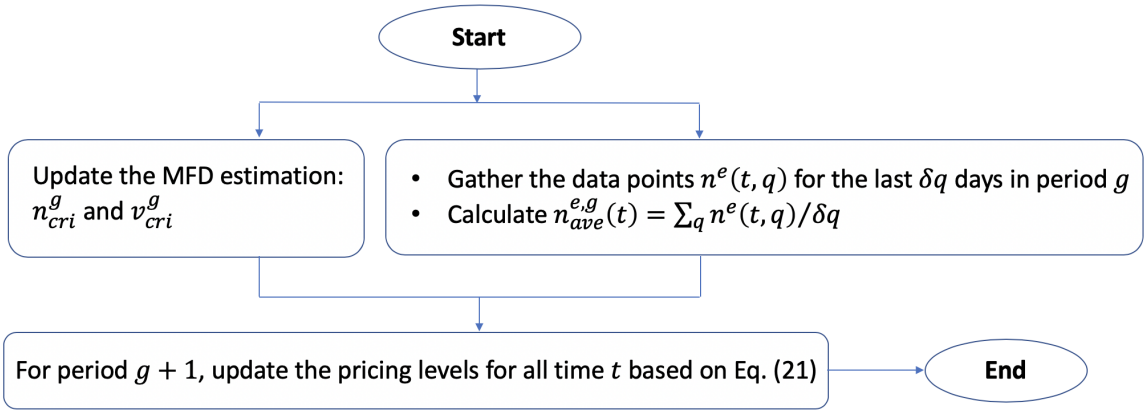

Figure 3: Procedure for determining the pricing adjustment

The adaptive pricing scheme tends to drive the region to operate at the critical accumulation (with minimum congestion and without capacity waste), where we decrease the pricing level during an un-congested duration and we increase the pricing level during a congestion duration. Operation at critical accumulation is generally beneficial, which has been discussed in the literature (Gonzales and Daganzo, 2012; Liu and Geroliminis, 2016).

It is worth mentioning here that for every t, we can define a different γ_t for it. However, for the ease of implementation, in practice, we should discretize the time horizon into multiple time intervals, and for each time interval, we should adopt the same price, and we can then define a time duration that is related to the pricing level updating for this time interval. The simplest case would be that the pricing level during one time interval would depend on only the conditions observed for this time interval itself. Our numerical studies later indicate that this simplest approach indeed already leads to significant efficiency gains.

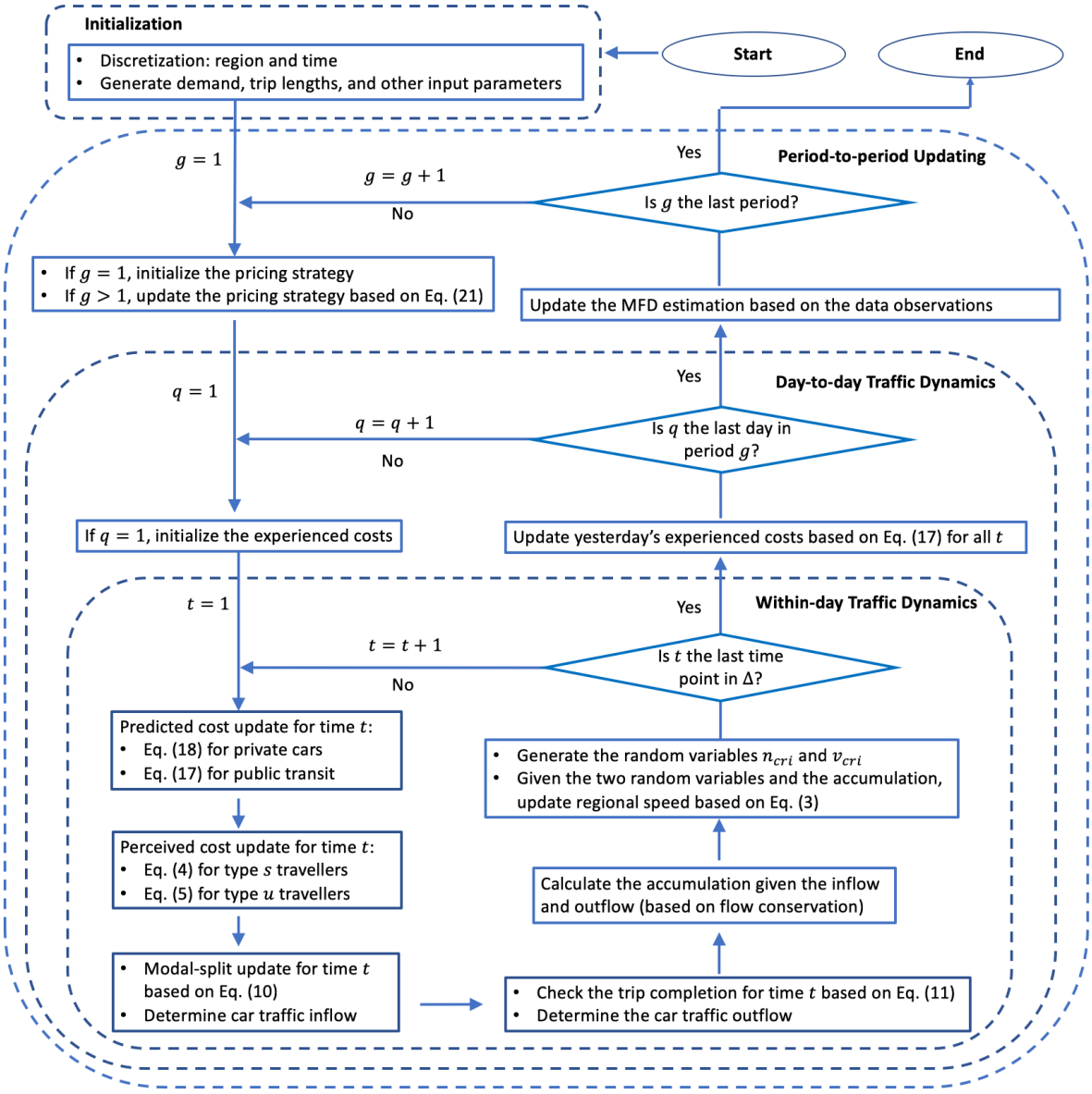

Figure 4: The overall framework

We summarize the combined framework for day-to-day traffic evolution and period-to-period MFD estimation and pricing adjustment in Figure 4. Note that the details for the MFD estimation and pricing adjustment have already been discussed earlier, where fewer details are included in Figure 4.

4 Numerical Studies

This section presents some numerical experiments to illustrate the proposed model. Particularly, we firstly describe the discretization of time and space for numerical experiments and list the benchmark numerical settings. Based on these, we then illustrate the day-to-day evolution process, the learning mechanism for the MFD, and the adaptive pricing scheme with numerical examples. In particular, we test how different levels of randomness in n_{cri} and v_{cri} may affect the bi-modal system dynamics, and the learning of MFD, and the adaptive pricing strategy. We also illustrate the impact of the penetration of smart information services. Moreover, we include some additional numerical results in Appendix B to further demonstrate the applicability of the proposed model in different contexts.

4.1 Numerical setting

We now present the numerical setting. Firstly, we describe the discretization of time and space and summarize some common parameters or variables in Table 1. Secondly, we provide the descriptions of the numerical settings for the public transit service, MFD uncertainty, the parameters involved in the MFD learning/estimation, and the setting for the adaptive pricing scheme. Thirdly, we describe the demand information, including demand intensity and trip lengths.

Table 1: Summary of basic numerical settings

Parameters or Functions	Specification
Transit fare, frequency, and speed	$p_b^w = 2$ (EUR/trip); $f_b^w = 10$ (veh/hr); $v_b = 25$ (km/hr);
Parameters for $v(n)$	$v_{cri} \sim \mathcal{U}(36, 44)$; $n_{cri} \sim \mathcal{U}(9000, 11000)$;
Value of time	$\alpha = 25$ (EUR/hr);
Learning parameters	$\eta_p = 0.5$; $\eta_e = 0.5$; $\eta_r = 0.8$;
Coefficient in the logit model	$\beta_m^w = 0.40$;
Proportions of the two types of users	$\theta = 0.75$; $1 - \theta = 0.25$;
Parameters for estimating the MFD	$\delta n = 50$ (veh); $\delta q = 5$ (days);
Coefficient for adaptive pricing	$p_{a,0}^w = 4 \times 10^{-4}$;

While the analytical model assumes the (clock) time and the space (location) to be continuous, for numerical analysis, the time horizon (within a day) is discretized into multiple small time intervals, and the city is discretized into multiple small areas. In particular, the

time horizon (within-day) $[0, \Delta]$ is discretized into M time intervals for each day, and the length of each interval is δt so that $M \cdot \delta t = T$. Specifically, we let $T = 4$ (hours) and $\delta t = 1$ (min), and thus $M = 240$. We consider a square city region with a size of 5km $\times$ 5km. The city is evenly divided into 25 small squares (sub-regions) with a size of 1km $\times$ 1km. Therefore, there are 25 origins and 25 destinations, and 25 $\times$ 25 O-D pairs. Note that the 'square city region' used here is a theoretical region and the data used to fit the MFD corresponds to simulated data.

We now provide some further discussions for the setting in Table 1. As can be seen, for the transit service, we consider a homogeneous service in the city region such that transit fare, frequency, and speed are identical (this is often the case in the city center region). Moreover, v_{cri} and n_{cri} are uniformly distributed within $\pm 10\%$ of the average values (we refer to it as "variation level" later in the paper), which are 40 and 10000, respectively. Later we will fix the mean value for both v_{cri} and n_{cri} and change the variation levels for sensitivity analysis. To facilitate reading, when we test the system with different levels of variations in n_{cri} and v_{cri}, we refer to it as "**Varying MFD Uncertainty**".

For estimating the critical parameters of the MFD, we let δn be 50 (for the moving average), which is 1% of the mean value for the critical accumulation n_{cri}. For the Nadaraya-Watson kernel regression based approach, the parameters utilized are specified in Section 3.3, where $h = 50$ (bandwidth for the Gaussian kernel) and $N = 1 \times 10^4$ (number of steps for discretizing the continuous variable "accumulation"). The data used for estimating the regional MFD comes from the observations (about speed and accumulation) in the numerical simulation from the past 15 days. The data used to estimate the average system performance under the given pricing strategy in a period comes from the last five days ($\delta q = 5$).

For the adaptive pricing, the price adjustment coefficient is $p^w_{a,0} = 4 \times 10^{-4}$. Note that this coefficient should be appropriately chosen in practice to avoid a big fluctuation (i.e., a too big coefficient) and to avoid non-effective price update (i.e., a too small coefficient). A reasonable coefficient may be obtained by comparing the relative magnitude of the toll level in practice to the average user travel delays in the network. More importantly, instead of adopting a different price for every time point, we divide the modeling duration into 8 time intervals (the length of each equals 30 minutes), and adopt the same price for a single time interval. Moreover, only the traffic conditions in a time interval are used for updating the pricing level in that time interval. Other parameters or settings, if not mentioned in Table 1, will be explicitly specified in the text.

Now we turn to the demand side, which is assumed to be identical for every day. The aggregate demand (relative intensity) profile over the clock time is displayed in Figure 5, where the modeling duration is 4 hours. Demand is relatively low outside the peak (before

$t = 0.4$h and after $t = 3.2$h), and demand is peaked in the middle of the duration for 1.6 hours. The demand distributions (relative intensity) over origin and destination are further displayed in Figure 6. As can be seen, demand intensity is higher if the origin is further away from the city center; and demand heading for the locations closer to the center is higher.

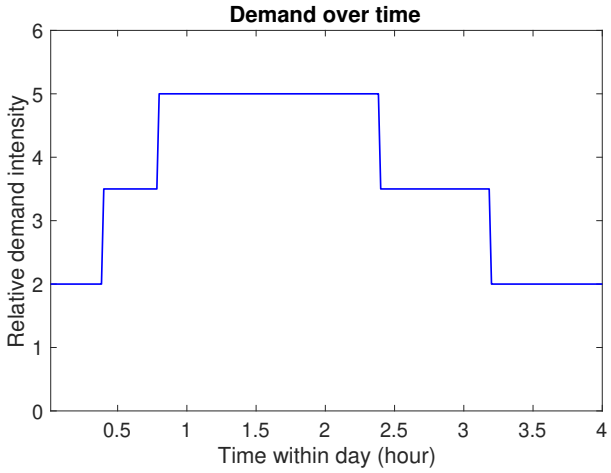

Figure 5: Travel demand pattern (relative intensity) over time (1=625 persons per minute)

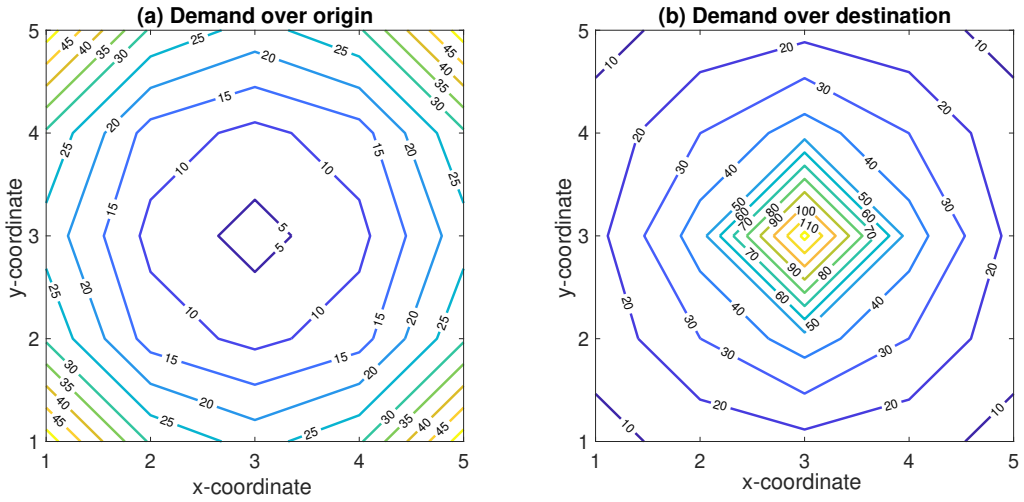

Figure 6: Travel demand pattern (relative intensity) over space

As the benchmark case, the proportions of type s and type u travelers are 75% and 25% (listed in Table 1), respectively. The value of 75% can be regarded as the penetration of real-time information services. To analyze how this penetration may affect system dynamics, we tested different values. To facilitate reading, we will refer to the case where we test the system with different penetrations of real-time information services as "**Varying Information Service Penetration**".

The trip length of travelers between a given O-D pair w is given as follows:

$$\begin{aligned} l_a^w &= \max\{1.6, 1.6 \cdot ||w||\} \\ l_b^w &= \max\{1.8, 1.8 \cdot ||w||\} \end{aligned}, \tag{22}$$

where $||w||$ is the Euclidean distance between the origin and the destination of O-D pair w. Note that the city was discretized into twenty-five 1km $\times$ 1km square areas in the numerical studies, and $||w||$ was measured based on the distance between the geometric centers of the origin and destination. The minimum values (1.6 and 1.8) for trip lengths in Eq. (22) are for trips within a single 1km $\times$ 1km square area or sub-region.[8] Moreover, we consider that $l_b^w > l_a^w$ as transit lines usually make detours to serve passengers from a large area.

To facilitate reading, we now summarize the two typical cases mentioned earlier: the **Varying MFD Uncertainty** case and the **Varying Information Service Penetration** case. In the **Varying MFD Uncertainty** case, the proportion of type s travelers (or the penetration of information services) was fixed at $\theta = 0.75$, but the variations in v_{cri} and n_{cri} changed from $\pm 0\%$ to $\pm 10\%$, and then to $\pm 20\%$, where $\pm 10\%$ is the benchmark level. In the **Varying Information Service Penetration** case, we fixed the variation at $\pm 10\%$ for both v_{cri} and n_{cri}. However, we changed the proportion of type s travelers (penetration of real-time information services), i.e., $\theta = 60\% \rightarrow 75\% \rightarrow 90\%$, where 75% is the benchmark level. Other numerical settings are identical.

4.2 Day-to-day evolution

Under the numerical setting in the above, we now examine the day-to-day stochastic traffic evolution process. For the benchmark case where the variations in n_{cri} and v_{cri} are within $\pm 10\%$ and the proportion of type s travelers (or the penetration of information service) is $\theta = 0.75$, we examine the evolution of car traffic inflow and outflow, the private car mode share, and the speed profile over both the clock time and the calendar time, which are shown in Figure 7. Note that the car traffic inflow and outflow and the private car mode share are aggregate values for all O-D pairs and all types of travelers.

[8] In this study, we consider the trips that have the same sub-region as both origin and destination. However, we do not consider the route choices of travelers (i.e., we do not consider which sub-regions a traveler may drive through to reach his or her destination). Also, traffic flow is governed by a single MFD for the whole region. Therefore, whether origin and destination sub-regions are the same or not does not affect the approach to modeling traffic dynamics. The only difference is that the trip lengths for different O-D pairs can be different. Recent studies have examined the estimation of regional trip length distributions, e.g., Batista et al. (2019).

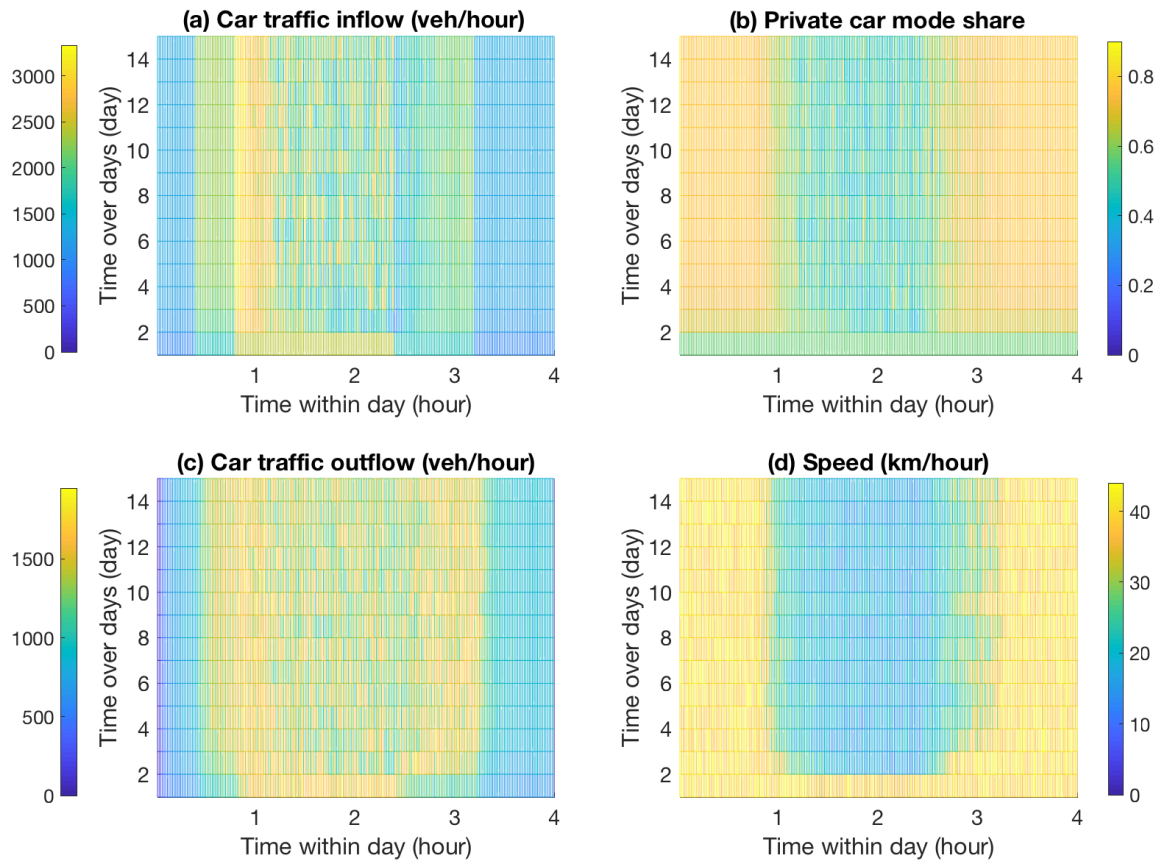

Figure 7: Evolution of modal-split, car traffic inflow and outflow, and speed over the clock time and the calendar time

In Figure 7, the x-axis and y-axis correspond to the clock time and the calendar time, respectively. There are several observations, which are explained as follows. Firstly, for the first two days (corresponding to 1 and 2 in the y-axis), the initial traffic condition of the system is far from traffic conditions in later days (e.g., day 11 to day 15). The inflow and outflow, the private car mode share, and the speed profile are thus much more different than those on the other days. As travel choices evolve over time, the system approaches similar conditions in later days. This is further verified by Figure 8, where we show the discrepancy between flows and costs for two consecutive days. Secondly, by comparing car traffic inflow with the speed profile, there is a (within-day) time-lag between inflow and congestion, i.e., the congestion follows after traffic inflow. Thirdly, the private car mode share is generally positively correlated with the speed profile. This is expected as a higher speed implies a lower travel time for travelers. Fourthly, during the most congested period (between hour 1 and hour 3), the outflow is at a medium level (marked by a mix of green and yellow in the

figure), which is indeed higher than that in the very un-congested period (before hour 0.5 and after hour 3.5). This is because during these very un-congested durations, travel demand is very low even if the private car mode share is high (please also refer to the demand profile in Figure 5).

To compare the flows and experienced costs for two successive days, i.e., we define the following discrepancy in system states for day $q'+1$:

$$\epsilon_{q'+1} = \frac{\int_t \sum_w \sum_m \left[\sum_k \frac{\left| r^w_{k,m}(t,q'+1) - r^w_{k,m}(t,q') \right|}{r^w_{k,m}(t,q'))} + \frac{\left| c^{e,w}_m(t,q'+1) - c^{e,w}_m(t,q') \right|}{c^{e,w}_m(t,q')} \right] dt}{2 \cdot |W| \cdot \Delta}. \tag{23}$$

The discrepancy in Eq. (23) is the summation of percentage errors for both realized flows and experienced costs (the first term and second term in the denominator in Eq. (23)), which is averaged over mode, O-D pair, and departure time. Note that alternatively we can evaluate $\epsilon_{q'+1}$ based on average flow and cost values, e.g., averages over 5 days; in this case, the magnitude of $\epsilon_{q'+1}$ is approximately reduced to $\frac{1}{5}$ of its value presented in this paper.

We fixed the proportion of type s travelers (or the penetration of information services) at $\theta = 0.75$ but changed the variations in v_{cri} and n_{cri} (with three levels: $\pm 0\%$, $\pm 10\%$, $\pm 20\%$, where $\pm 10\%$ is the benchmark level), i.e., the **Varying MFD Uncertainty** case. Specifically, Figure 8 shows the evolution of the discrepancy defined by Eq. (23) for the system under different levels of variations. As can be seen, when the variation is smaller, the discrepancy can approach smaller values with a faster speed (a smaller discrepancy value given the same calendar time). This is expected as when the uncertainty of network performance is smaller, the traffic patterns in the network approach more similar states for consecutive days after a certain period of the traveler learning process.

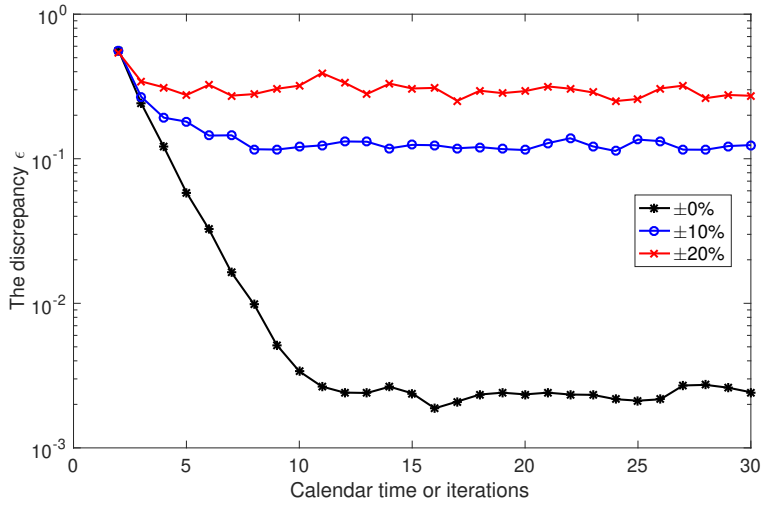

Figure 8: Evolution of ϵ over the calendar time under different variations in v_{cri} and n_{cri}

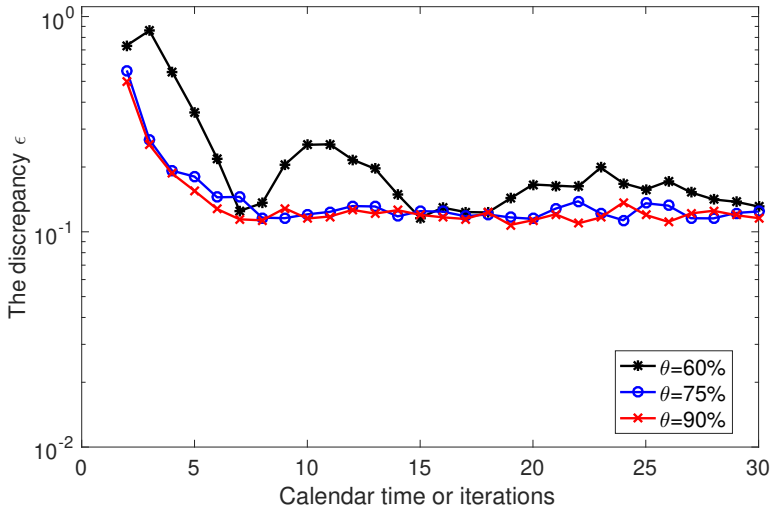

Figure 9: Evolution of ϵ over the calendar time under different values of θ

We fixed the variation at ±10% for both v_{cri} and n_{cri} as described in Table 1. However, we changed the proportion of type s travelers (penetration of real-time information services), i.e., $\theta = 60\% \rightarrow 75\% \rightarrow 90\%$, i.e., the **Varying Information Service Penetration** case. Figure 9 displays the discrepancy defined by Eq. (23) for the system under different values of θ (note that the benchmark value is 75%). As can be seen, when θ is larger ($75\% > 60\%$ and $90\% > 60\%$), generally the system approaches more similar states in a faster way (a smaller discrepancy value given the same calendar time). However, while the penetration is already relatively large (i.e., $\theta = 75\%$), the reduction in the discrepancy (in the average sense) becomes marginal if we further increase θ (see the case with $\theta = 90\%$).

4.3 Learning of an MFD and the period-to-period pricing

In this section, we firstly examine the learning of an MFD and then illustrate the adaptive pricing scheme. We start with illustrating the learning of an MFD. Particularly, we explore the learned curve $v'(n)$ against the observed values. An example of the observed data for each of the relationships $v - n$ and $v(n) \cdot n - n$ is shown in Figure 10, where the variations are within $\pm 10\%$.

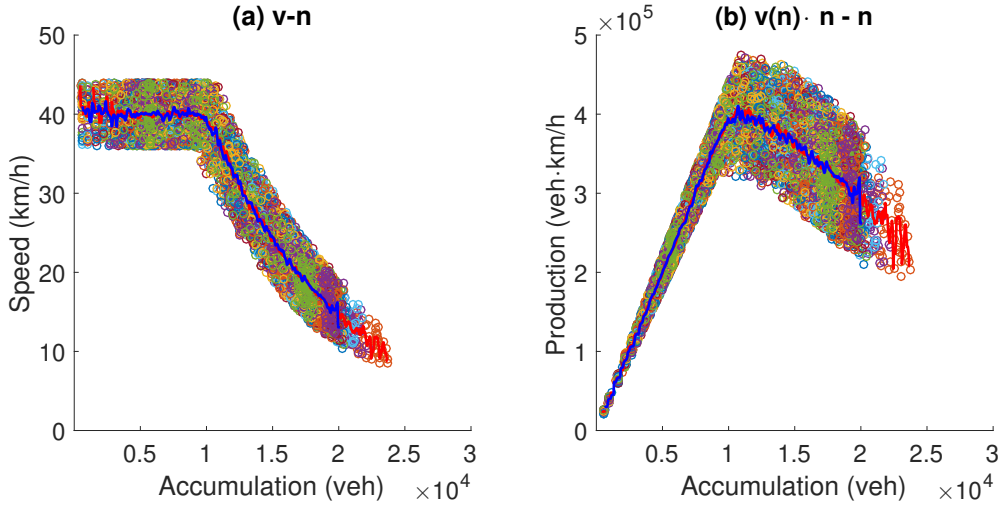

Figure 10: Observations for estimating an MFD (for 15 days)

In Figure 10, the circles are observations from different days (with different colors), the blue solid line is the weighted average based on Nadaraya-Watson kernel regression, and the red solid line is the simple moving average. These two estimates are close to each other while the weighted average based on Nadaraya-Watson kernel regression appears to be slightly smoother. Later we will only present the results based on the weighted averages.

The determination of n_{cri} and v_{cri} can be updated over days once new observations become available, for which an example is shown in Figure 11 under different levels of uncertainty $(\pm 0\%, \pm 10\%, \pm 20\%)$, i.e., we again look at the **Varying MFD Uncertainty** case.

Particularly, Figure 11 displays the estimated n_{cri} and v_{cri} over the calendar time. Note that while these estimations can be updated on each day, it does not mean that the pricing level is updated every day (indeed the pricing level is updated from period to period and each period contains 15 days in the example). As one can see from Figure 11, the estimations tend to approach a constant value after a number of days/iterations. Moreover, when the variation is larger $(\pm 0\% \to \pm 10\% \to \pm 20\%)$, the estimation deviates more from the expectation. It is further observed that for a variation level of $\pm 20\%$, the variation interval is indeed 40%

of the mean value (for both v_{cri} and n_{cri} simultaneously). The relative error for the critical accumulation estimation approaches a value less than 20%. A similar trend can be observed for the critical speed estimation, which can be seen from Figure 11. Moreover, similar observations can be identified for a variation level of ±10%.

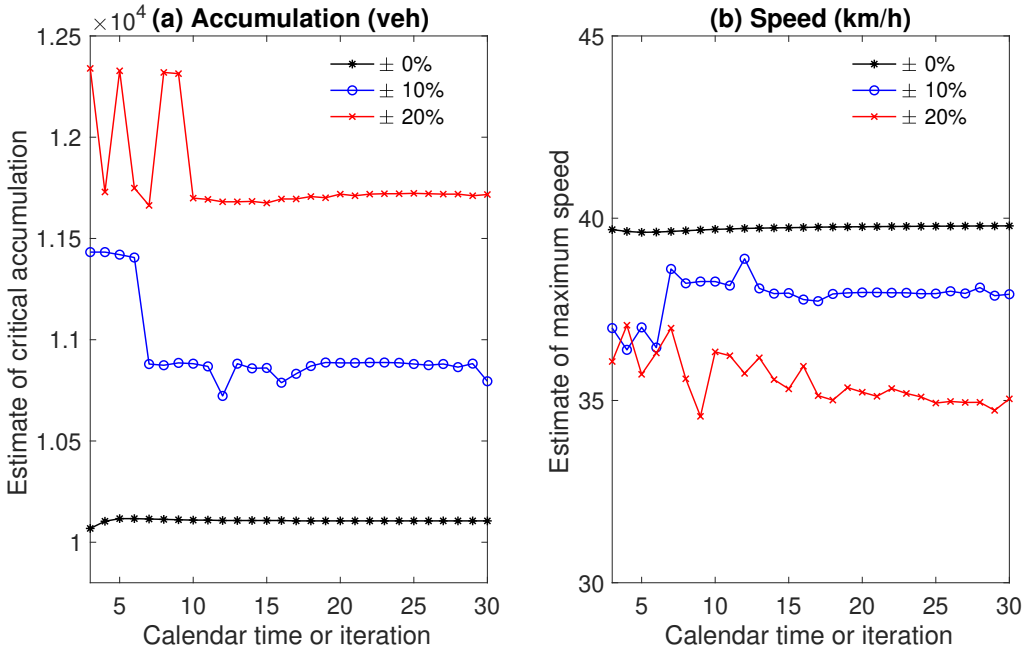

Figure 11: Evolution of the estimations for critical speed and accumulation

There are two additional observations from Figure 11 for the non-parametric estimation approach. Firstly, the critical accumulation tends to be overestimated and the critical speed tends to be underestimated accordingly. This is related to the speed functional form in Eq. (3), which is briefly explained as follows. The non-parametric estimation approach tries to identify an accumulation value with the largest production $v(n) \cdot n$. The overestimation of n_{cri} (an n larger than the true mean of n_{cri}) is more likely to yield a larger $v(n) \cdot n$. This is because, when the value of n_{cri} increases from its mean, for an n smaller than the mean of n_{cri}, the speed $v(n)$ remains the same (equal to v_{cri} based on Eq. (3)). However, for an n larger than the mean of n_{cri}, the speed $v(n)$ increases with respect to n_{cri} (when compared to the case with n_{cri} equals its mean), and the production $v(n) \cdot n$ increases accordingly. This is the dominating factor for us to have a larger production value for an n slightly larger than the mean of n_{cri}. This can be seen from Figure 10b (the maximum production occurs when accumulation is larger than 1×10^4, i.e., the mean of n_{cri}). Given an overestimated n_{cri}, we have an underestimated $v_{cri} = E(v(n_{cri}))$. Secondly, even if we have ±0% variations for n_{cri} and v_{cri}, the estimations still deviate a bit from the exact values and can fluctuate slightly

over days/iterations. This is due to the following: (i) the speed functional form is assumed unknown for the estimation process; (ii) there is a non-differentiable and non-smooth point at n_{cri} for the speed-accumulation curve; (iii) sets of observations used for estimations on different days/iterations are slightly different.

We now turn to the period-to-period adaptive pricing. Before moving further, we here summarize several efficiency measures of our interest. Firstly, the total (experienced) cost of all travelers can be written as

$$TC = \int_t \sum_w \sum_m \left[c_m^{e,w}(t) \cdot \sum_k r_{k,m}^w(t) \right]. \tag{24}$$

Similarly, we can write down the total pricing charges and total transit revenues as follows:

$$TP_m = \int_t \sum_w \left[p_m^w(t) \cdot \sum_k r_{k,m}^w(t) \right], \tag{25}$$

where $m = a$ for the pricing charges and $m = b$ for the transit fares. The total social/system cost can then be determined by

$$TSC = TC - \sum_m TP_m. \tag{26}$$

Note that the monetary cost is considered a transfer of money rather than social cost. Moreover, the operating cost of transit is not included here. However, as public transit provides the same service for each O-D pair from day to day, the operating cost is identical and its exclusion does not affect the overall pattern of the total system cost.

For the period-to-period adaptive pricing, we let the period length be 15 days. We then simulated the day-to-day evolution process and the pricing adjustment process (pricing adjustment occurs at the beginning of each period). Moreover, we set the initial pricing level $p_a^w(t) = 2$(EUR) for all departure times and O-D pairs, which is equal to the transit fare. We then explored the evolution of pricing levels, bi-modal system performance, and speed profiles over time (both the clock time and the calendar time).

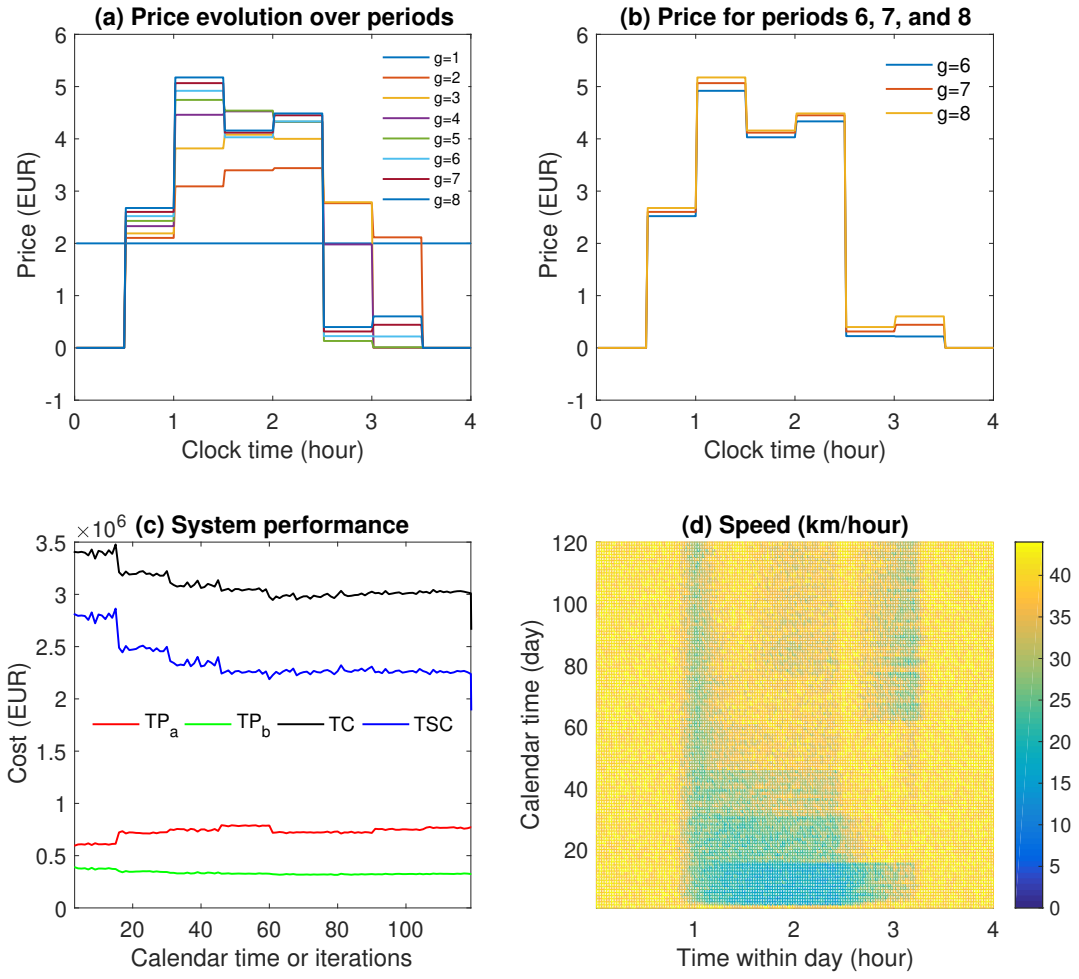

Figure 12: Evolution of pricing levels, system efficiency, and speed profile

Figure 12 displays the evolution of pricing levels over periods and the corresponding system performance and speed profile for the case with the variation within $\pm 10\%$. Particularly, Figure 12a shows the prices for the eight periods of our interest while Figure 12b shows the prices for the last three periods. As one can see, the time-dependent pricing levels approached in the later periods are temporally compatible with the time-dependent demand and observed traffic conditions. This helps to improve system efficiency, e.g., the total system cost TSC was reduced from 2.81×10^6 (at the beginning of the first period) to 2.24×10^6 (at the end of the last period), which is around 20% of the cost under the initial flow pattern, as shown in Figure 12c. Note that a period has 15 days and efficiency metrics (e.g., TC and TSC) have relatively sharp changes after every 15 days (due to the pricing adjustment). It is also noteworthy that the total cost of travelers TC is reduced through pricing. This is

due to the reduction in (hyper)congestion. Similar results were observed by Geroliminis and Levinson (2009) and Liu and Geroliminis (2016). Furthermore, Figure 12d shows the corresponding speed profile under the adaptive pricing in Figure 12a, where the x-axis is the clock time and the y-axis is the calendar time (thus we present both day-to-day and within-day dynamics). As can be seen, for the first period (the first 15 days) when the pricing levels are far from the levels approached in later periods, there is significant congestion between $t = 1$h and $t = 3$h, which is temporally compatible with the demand pattern depicted in Figure 5. Starting from the second period (i.e., from day 16), with the adjustment of pricing levels in Figure 12a, the congested duration becomes shorter (the duration with green color becomes shorter) and the congestion becomes less severe (for some time intervals, the green color becomes light even if it is still green). Moreover, it can be seen that the speed profile (within-day) approaches a similar time-dependent pattern at the end of a period (the pricing levels remain the same within a period), although the exact speed profile varies from day to day due to the stochastic traffic dynamics. This is consistent with the observations in Figure 8.

Figure 13 further illustrates the pricing levels and the system performance after we varied the levels of uncertainty (i.e., $\pm 0\%$, $\pm 10\%$, $\pm 20\%$), i.e., the **Varying MFD Uncertainty** case. We omit the results for the pricing level and speed profile as they appear to be very similar (but with minor differences). For the corresponding total system cost, we can observe from Figure 13 that when the variations are different, the adaptive pricing scheme leads to similar system performance (slightly different under different levels of variations), while the size of variations of system performance is compatible with that of n_{cri} (and v_{cri}).

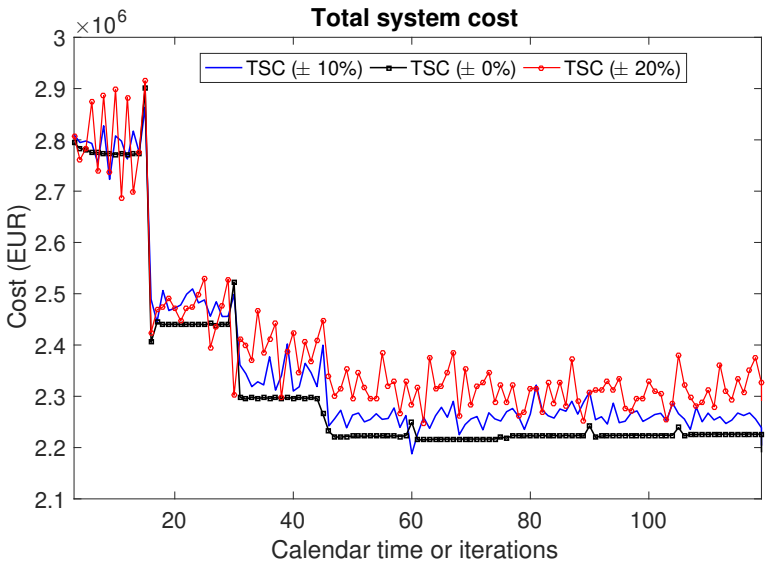

Figure 13: Evolution of total system costs given different levels of uncertainty

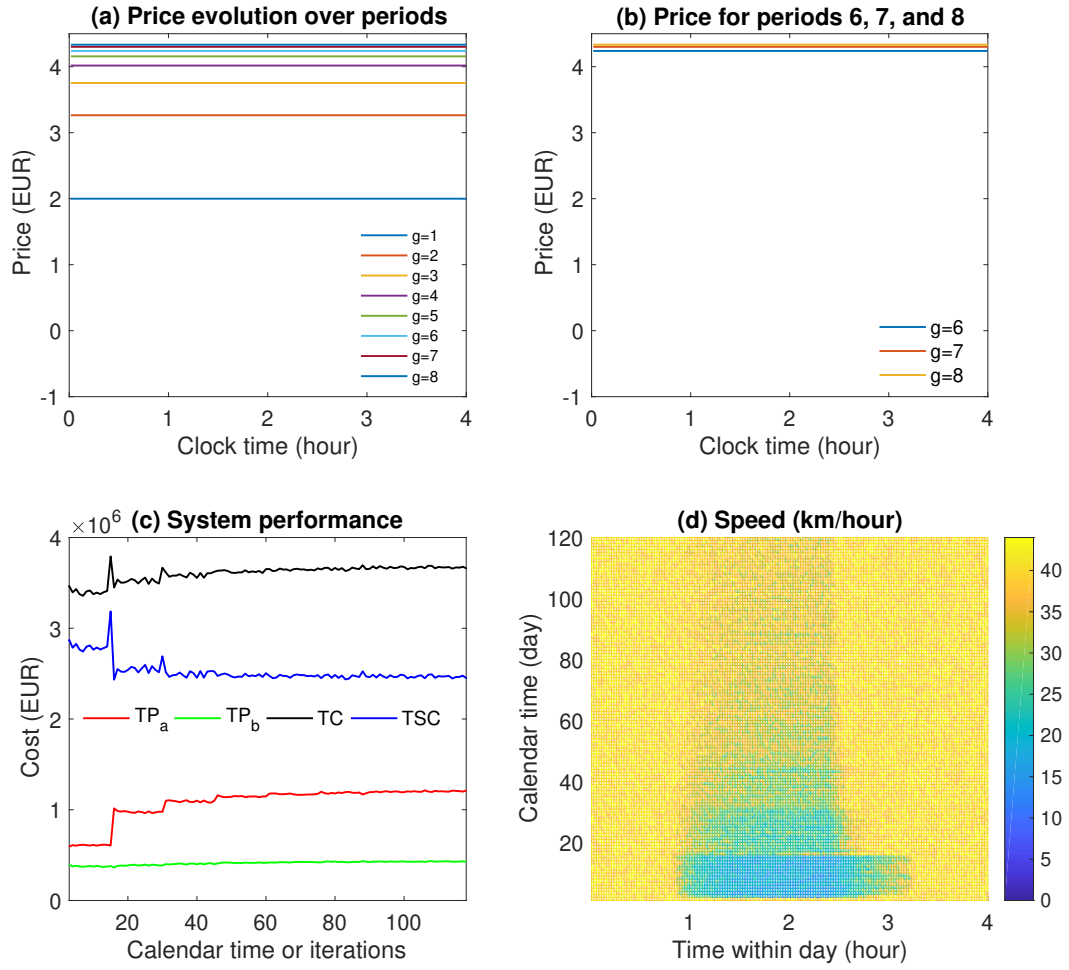

Figure 14: Evolution of total system costs under adaptive and constant pricing

Figure 14 displays the evolution of pricing levels over periods and the corresponding system performance and speed profile for the case with constant pricing (over the clock time) when the variations are still within $\pm 10\%$ for n_{cri} and v_{cri}, which are similar to those for the dynamic pricing case in Figure 12. By comparing Figure 12 and Figure 14, we can conclude that the proposed adaptive pricing scheme with constant pricing still helps improve system efficiency (Figure 14c) and eliminate congestion (Figure 14d). However, it loses efficiency when compared with dynamic pricing, which is shown in Figure 14c, where the cost achieved in later periods is approximately 2.48×10^6. This efficiency loss ($(0.24 = 2.48 - 2.24) \times 10^6$) is around 9% of the total cost under the initial flow pattern, which is due to the inability of the constant pricing to capture demand variations over (the clock) time. This highlights the need of the time-dependent pricing strategy. Moreover, by comparing Figure 14d and Figure 12d,

we further have the following observations. At the end of period 8, in the case with time-dependent pricing, since pricing levels are different for different time intervals (within-day), the distribution of congestion over time is relatively uneven, e.g., in Figure 12d green colors appear around $t = 1$h (when the demand level starts to be relatively high) and $t = 3$h (when the demand level starts to be relatively low) while yellow colors dominate between $t = 1.2$h and $t = 2.8$h. Differently, for the case with constant pricing, since the same relatively high pricing level applies to all time intervals with different demand levels at the end of period 8, as long as the time interval with the peak demand (refer to Figure 5) does not involve too much congestion, the other time intervals with lower demand levels do not involve too much congestion.

5 Conclusion

This paper proposes a framework for modeling and managing stochastic traffic dynamics in a bi-modal transportation system. The study has several key features. Firstly, we embed the network-level stochastic within-day traffic dynamics into the day-to-day framework and develop a stochastic doubly dynamical system. Secondly, time-dependent traffic conditions and information provision are incorporated in the travelers' decision process, where both travelers with and without information are modeled. Thirdly, a learning mechanism for the MFD of the network is developed, which can take advantage of the day-to-day traffic observations. Fourthly, the learned MFD is coupled with an adaptive and time-dependent pricing strategy. The learning and managing framework holds potential to adaptively enhance network performance.

This study can be further extended in several avenues. Firstly, in this paper while we extend the study of Liu and Geroliminis (2017) by considering a two-dimensional city, we do not consider the route choice of travelers. Future research can extend the modeling framework in this paper to include their route choices. Secondly, the travel demand over time is assumed to be fixed (but time-dependent) and the departure time choice is not modeled. We may include the activity schedules of travelers and explore the trip-timing choices in the doubly dynamical system developed. Thirdly, this study assumes a dedicated right-of-way for the public transit system. Therefore, the direct interaction between private car and public transit is ignored. If this interaction is to be considered, 3D-MFD models can be utilized. In this case, how to appropriately estimate the stochastic 3D-MFD will be a challenging issue since more random variables have to be accommodated. The pricing mechanism has also to be modified to accommodate the 3D-MFD. Fourthly, the real-time information service considered in this paper is just one simple and widely used way of information services. In

the future, we shall consider different types of smart services and model how they affect travelers' learning and decision process. Fifthly, due to the complexity of the within-day stochastic traffic dynamics, it is extremely difficult if not impossible to analytically explore the properties of the stochastic dynamical process. Future research will look into this issue by, e.g., simplifying the traffic dynamics, the network setting, or the demand setting. Furthermore, in this paper, the learning parameters in the travelers' learning mechanism are constant over time. However, these parameters may be changing over time. Techniques from the reinforcement learning literature can be utilized to accommodate it. In particular, one may expect that travelers' learning can improve over time. We will look into these issues in a systematic manner in our future study.

Acknowledgment. We would like to thank the anonymous reviewers for their very thoughtful and helpful comments, which have helped improve both the technical quality and exposition of the paper. The work described in this paper was partially supported by a grant from the Hong Kong Research Grants Council (HKU17218916), and a grant from the University Research Committee, The University of Hong Kong (201711159034). Dr. Wei Liu would like to thank the Principal's Early Career Mobility Fund from the University of Glasgow, which initiated this research. A significant part of this paper was completed after Dr. Wei Liu moved to the University of New South Wales, Sydney.

Appendix A. Notations

Table 2: List of main notations

Notations	Specification
$c_{k,m}^{p,w}(t,q)$	The mean perceived travel cost of type k travelers between O-D pair w who depart at time t and choose mode m on day q
$\mathbf{c}_k^p(t,q)$	$=\left\{c_{k,a}^{p,1}(t,q), c_{k,b}^{p,1}(t,q), ..., c_{k,a}^{p,\lvert W\rvert}(t,q), c_{k,b}^{p,\lvert W\rvert}(t,q)\right\}^T$ is the vector of the mean perceived travel costs, where W is the set of all O-D pairs and $\lvert W\rvert$ is the total number of O-D pairs
$c_m^{e,w}(t,q)$	The experienced travel cost of travelers between O-D pair w who depart at time t and choose mode m on day q
$\mathbf{c}^e(t,q)$	$=\left\{c_a^{e,1}(t,q), c_b^{e,1}(t,q), ..., c_a^{e,\lvert W\rvert}(t,q), c_b^{e,\lvert W\rvert}(t,q)\right\}^T$ is the vector of experienced travel costs

$c_m^{r,w}(t,q)$	The predicted travel cost of travelers between O-D pair w who depart at time t and choose mode m on day q
$\mathbf{c}^r(t,q)$	$=\left\{c_a^{r,1}(t,q), c_b^{r,1}(t,q), ..., c_a^{r,\|W\|}(t,q), c_b^{r,\|W\|}(t,q)\right\}^T$ is the vector of predicted travel costs
f_b^w	Public transit frequency between O-D pair w
g	The period index, where a period consists of a number of days (for the period-to-period model)
h	The bandwidth for the Gaussian kernel
H	The set of all data points $\{(v_a^e(t,q), n^e(t,q))\}$ over (t,q)
H_n	The set of data points $\{(v_a^e(t,q), n^e(t,q))\}$ over (t,q) where $\|n^e(t,q)-n\| \leq \delta n$
$k \in \{s,u\}$	The user type, where $k=s$ represents the user type with smart information services and $k=u$ represents the user type without smart information services
l_m^w	The trip length for mode m and O-D pair w
$m \in \{a,b\}$	Travel mode, where $m=a$ represents the private car mode and $m=b$ represents the public transit mode
n	Accumulation: the total amount of traffic in a region
n_{cri}	The critical accumulation, where the production $v(n)\cdot n$ is maximized
n_{cri}^g	The estimated critical accumulation for period g
$n^e(t,q)$	The realized regional accumulation at time t on day q
$n_{ave}^{e,g}(t)$	The average value of accumulation at time t over a number of days at the end of period g
N	The number of steps for discretizing the accumulation
$o^w(t)$	The total amount of car traffic between O-D pair w arriving at the destination at time t
$O^w(t)$	The cumulative car traffic between O-D pair w arriving at the destination before or at time t
$p_m^w(t)$	The monetary cost for travelers between O-D pair w who depart at time t and choose mode m
$p_m^w(t,g)$	The monetary cost for travelers between O-D pair w who depart at time t and choose mode m in period g
$p_{a,0}^w$	A coefficient for pricing adjustments
$Pr_{k,m}^w(t,q)$	The proportion of type k travelers between O-D pair w who depart at time t and choose mode m on day q
q or q'	The calendar time, i.e., the day index (for the day-to-day model)
$r^w(t)$	The total travel demand between O-D pair w departing at time t

$r_k^w(t)$	Type k travel demand between O-D pair w departing at time t, where $r_k^w(t) = \theta_k \cdot r^w(t)$
$r_{k,m}^w(t)$	Type k travel demand for mode m, O-D pair w, departure time t, where $\sum_m r_{k,m}^w(t) = r_k^w(t)$
$r_{k,m}^w(t,q)$	The realized $r_{k,m}^w(t)$ on day q
$\mathbf{r}(t,q)$	$=\left\{r_{s,a}^1, r_{s,b}^1, ..., r_{s,a}^{\lvert W\rvert}, r_{s,b}^{\lvert W\rvert,}, r_{u,a}^1, r_{u,b}^1, ..., r_{u,a}^{\lvert W\rvert}, r_{u,b}^{\lvert W\rvert}\right\}^T$ is the vector of the realized travel demand. Note that (t,q) is omitted inside the vector expression to ease the notation, and $\lvert W\rvert$ is the total number of O-D pairs.
$R_{k,a}^w(t)$	Cumulative car inflow of type k travelers between O-D pair w and with departure time t, where $\sum_m r_{k,m}^w(t) = r_k^w(t)$
$\mathbf{R}(t)$	$= \left\{r^1(t), r^1(t), r^2(t), r^2(t), ..., r^{\lvert W\rvert}(t), r^{\lvert W\rvert}(t)\right\}^T$ is the total demand column vector for the total travel demand departing at time t
t or $t^{'}$	The (clock) time (for the within-day model)
$T_m^w(t)$	Travel time for travelers between O-D pair w who depart at time t and choose mode m
$v(\cdot)$	The regional speed function for car traffic
v_{cri}	The critical speed, where $v_{cri} = v(n_{cri})$
v_a	The regional space-mean speed for car traffic
$v_a^e(t)$	The realized regional (car) traffic speed at time t
$v_a^e(t,q)$	The realized regional space-mean speed at time t on day q
v_b	The transit speed
w or w'	An O-D pair
W	The set of all O-D pairs, where $w, w' \in W$
(x,y)	A point with the coordinates of x and y in the Cartesian coordinate system, which can be either an origin or a destination
z_1 and z_2	Parameters to be determined in the discrete-time approximation for travel time
α	The value of time
β_m^w	The coefficient in the Logit choice model for mode m and O-D pair w
γ_t	A duration defined for time t, where $t \in \gamma_t$
δn	The interval length used for discretizing the accumulation n
δq	A number of days: during which traffic data is used to measure system performance
Δ	$[0, \Delta]$ is the modeling duration within a day
ε_m^w	The random term associated with the mean perceived cost $c_{k,m}^{p,w}(t,q)$
η_e, η_p, η_r	The coefficients associated with the experienced cost, mean perceived cost, and predicted cost in the equation for travelers' perception updating

θ_k	The proportion of type k travelers among $r^w(t)$
τ	The (clock) time (for the within-day model)
$\Phi_{k,m}^w(\cdot)$	The modal-split function for type k travelers between O-D pair w who choose mode m
$\Phi_k(\cdot)$	$=diag\left\{\Phi_{k,a}^1(\cdot), \Phi_{k,b}^1(\cdot), ..., \Phi_{k,a}^{\lvert W\rvert}(\cdot), \Phi_{k,b}^{\lvert W\rvert}(\cdot)\right\}^{2\lvert W\rvert\times 2\lvert W\rvert}$ is the modal-split matrix, where $\lvert W\rvert$ is the total number of O-D pairs
Ω	The feasible flow set defined in Eq. (1): $\left\{r_{k,m}^w(t) \geq 0, \forall k, m, w, t\right\}$

Appendix B. Extended Numerical Results

Now we provide some further numerical tests to show the applicability of the proposed model in different contexts. Moreover, we use a different approach to estimate the critical accumulation and speed, where the speed-accumulation functional form is utilized.

Appendix B1. MFD Learning: Varying Variability for n_{cri} and v_{cri}

Firstly, we explore the case when the randomnesses of n_{cri} and v_{cri} can change from day to day. We consider that the average values of n_{cri} and v_{cri} remain constant, while the exact distributions of n_{cri} and v_{cri} vary over days. In this context, Figure 15 displays the estimations for critical speed and accumulation over calendar time, which is comparable to Figure 11 (where the distributions of n_{cri} and v_{cri} do not vary from day to day). In Figure 15, the star-marked line corresponds to the case where on each day the probability for a level of uncertainty $\pm 0\%$ is 0.5, and that for $\pm 10\%$ is also 0.5 (for both n_{cri} and v_{cri}); the circle-marked line corresponds to the case where on each day the probability for a level of uncertainty $\pm 10\%$ is 0.5, and that for $\pm 20\%$ is 0.5. All other numerical settings are identical to those in Section 4.

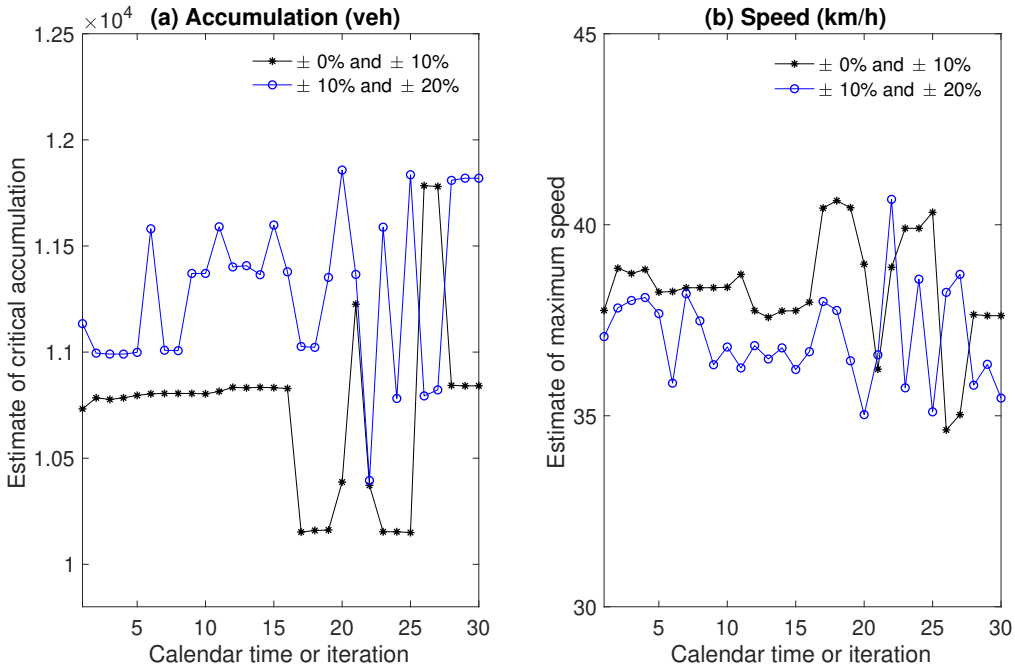

Figure 15: Evolution of the estimations for critical speed and accumulation with varying uncertainty levels

By comparing Figure 15 with Figure 11, we have three key observations. Firstly, one can readily identify that when the distributions of n_{cri} and v_{cri} vary from day to day, there are more fluctuations in the estimated values. Secondly, a combination of $\pm 0\%$ and $\pm 10\%$ indicates smaller variations in n_{cri} and v_{cri} than that of $\pm 10\%$ and $\pm 20\%$, meaning that the estimated values for the former are more accurate (on average). Thirdly, a combination of $\pm 0\%$ and $\pm 10\%$ shows larger variations than $\pm 0\%$ but smaller variations than $\pm 10\%$, meaning that the estimated values on average are less accurate than those for $\pm 0\%$ and more accurate than those for $\pm 10\%$. Similar trends can be observed for a combination of $\pm 10\%$ and $\pm 20\%$.

Appendix B2. MFD Learning: An Explicit Approach

We now consider that when we estimate the speed-accumulation and/or production-accumulation curve, the speed function in Eq. (3) is known and explicitly utilized. We then only need to calibrate two parameters n_{cri} and v_{cri} for the speed-accumulation function.

We have all data points $(v_a^e, n^e) \in H$. We solved the following minimization problem:

$$\min_{(n_{cri}, v_{cri})} \sum_{(v_a^e, n^e) \in H} \left[v_a^e - v\left(n^e\right) \right]^2, \tag{27}$$

where $v(\cdot)$ is given in Eq. (3).

By adopting the above approach, Figure 16 displays the estimated n_{cri} and v_{cri} over the calendar time. Similar to Figure 11, three levels of uncertainty are considered, i.e., $\pm 0\%$, $\pm 10\%$, and $\pm 20\%$. Moreover, all other numerical settings are identical to those in Section 4 when generating traffic patterns from day to day. By comparing Figure 16 with Figure 11, we have three key observations. Firstly, for the current explicit estimation approach, the estimated values sometimes change very little from day to day, and sometimes change relatively significantly. Overall, there are more fluctuations in the estimated values. This is explained as follows. The optimization problem in Eq. (27) tries to minimize the error terms for speed observations. When new observations differ significantly from the average, the optimization problem tends to adjust the estimated n_{cri} and v_{cri} more sharply. Secondly, as discussed in Section 4.3, the non-parametric approach proposed tends to overestimate the critical accumulation and underestimate the critical speed. However, the current explicit approach is arbitrary. Thirdly, when the variations in n_{cri} and v_{cri} are smaller, the estimations are more accurate with the explicit approach. This is similar to the proposed non-parametric approach. In the case of $\pm 0\%$ variation, the estimation is perfectly accurate with the explicit approach. However, for the non-parametric approach, the estimations still deviate a bit from the exact values even if we have $\pm 0\%$ variations.

It is worth mentioning that the explicit approach considered here gives estimations with more fluctuations, but the relative accuracy of the estimated values is comparable to that of the proposed non-parametric approach. However, this only occurs when we know the exact and correct functional form for the speed-accumulation function. If we adopt a "wrong" form for the speed-accumulation function, the explicit approach can result in very large discrepancies. We omit detailed numerical illustrations to save space.

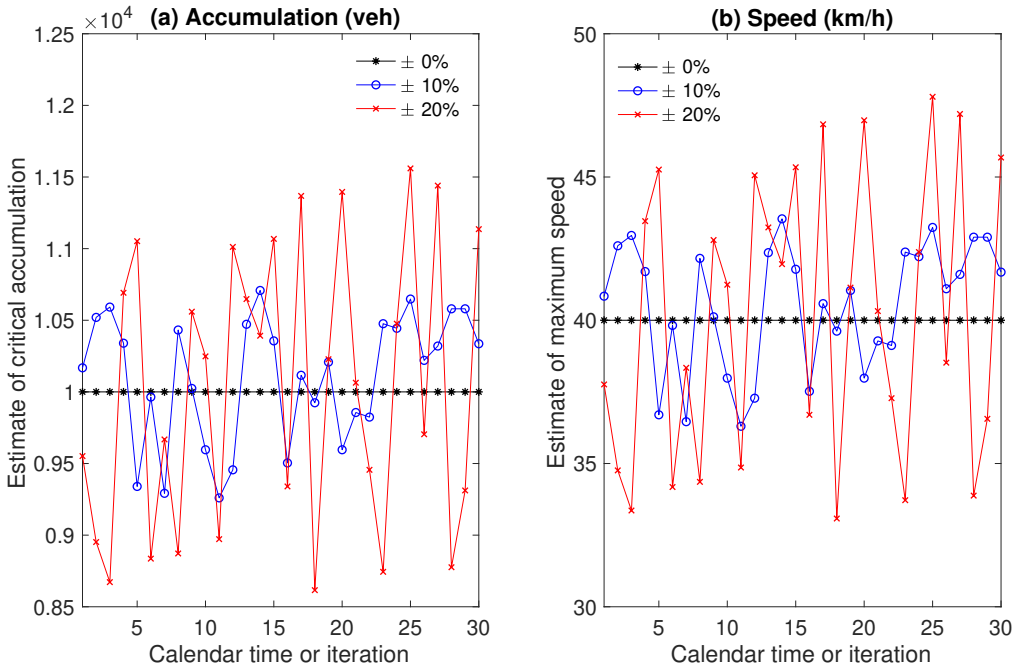

Figure 16: Evolution of the estimations for critical speed and accumulation with a closed-form approach

Appendix B3. Extended Numerical Results for the Northwestern Speed Model Case

Generally speaking, the modeling framework in this paper does not rely on the speed-accumulation specification in Eq. (3). To illustrate this, we examine the case with the Northwestern Model (Drake et al., 1965), which is given as follows:

$$v\left(n\right) \equiv v_{cri} \cdot e^{-\frac{1}{2}\cdot\left(\frac{n}{n_{cri}}\right)^2}. \tag{28}$$

We adopted the uniform distributions for the two parameters in the speed function, $v_{cri} \sim \mathcal{U}(45, 55)$ and $n_{cri} \sim \mathcal{U}(9000, 11000)$, as the benchmark case (i.e., $\pm 10\%$ variation for both n_{cri} and v_{cri}). All other numerical settings are identical to those in Section 4.1.

Figure 17 shows the estimations for critical speed and accumulation over calendar time. Similar to Figure 11, with unchanging average values for n_{cri} and v_{cri} , three levels of variations were examined, i.e., $\pm 0\%$, $\pm 10\%$, and $\pm 20\%$, where $\pm 10\%$ is the benchmark case. It is evident that a smaller level of variation results in a more accurate estimation (closer to the real average value). Moreover, the estimated value for the maximum speed varies very little from day to day, which is different from that under the speed function in Eq. (3). This

is because, for Eq. (28), v_{cri} is the critical/maximum speed occurring at $n = 0$. Therefore, the estimation of v_{cri} can be simply based on observations at $n = 0$. For Eq. (3), v_{cri} is the speed at $n = n_{cri}$, i.e., $v_{cri} = v(n_{cri})$. Since n_{cri} also varies, the estimated v_{cri} fluctuates more.

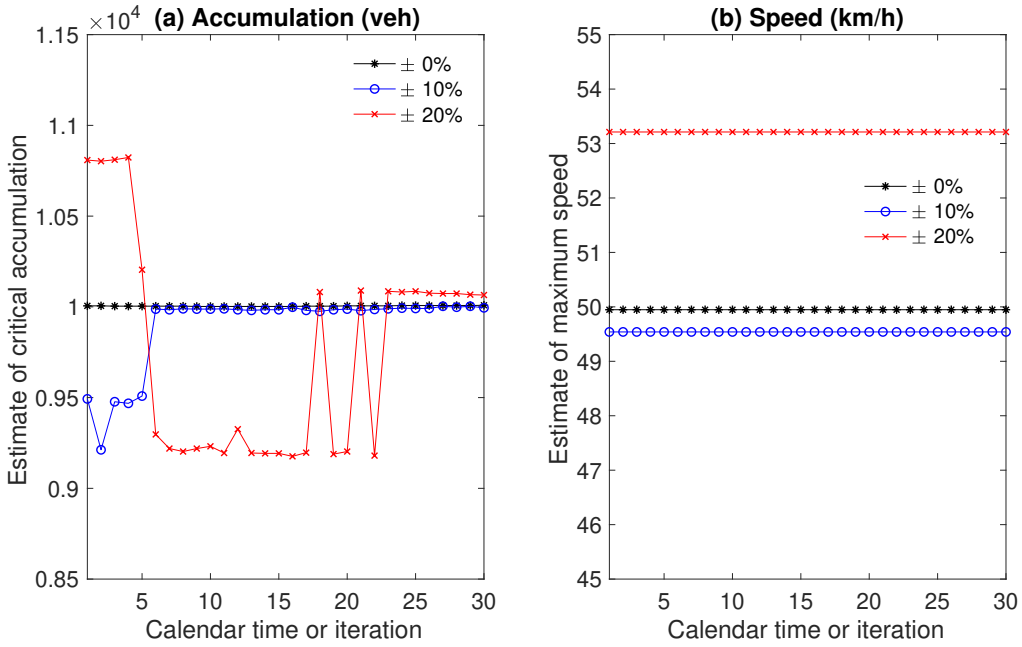

Figure 17: Evolution of the estimations for critical speed and accumulation: the Northwestern speed model case

Similar to Section 4.3, we now examine the period-to-period adaptive pricing. Figure 18 displays the evolution of pricing levels over periods (Figure 18a and Figure 18b) and the corresponding system performance (Figure 18c) and speed profile (Figure 18d) for the benchmark case with a level of variation at ±10%. These results are consistent with those in Section 4.3 with a different speed function. Particularly, in the current case, the total system cost was reduced from 3.293×10^6 to 2.630×10^6 through the adaptive pricing. It is worth mentioning that the speed profile in Figure 18d does not approach the maximum speed for the peak demand duration (between $t = 0.5h$ and $t = 3.2h$ in Figure 5). This is because the production (i.e., $n \cdot v(n)$) is maximized at $n = n_{cri}$, where the speed based on Eq. (28) (around $30km/h$) is less than the maximum speed (around $50km/h$).

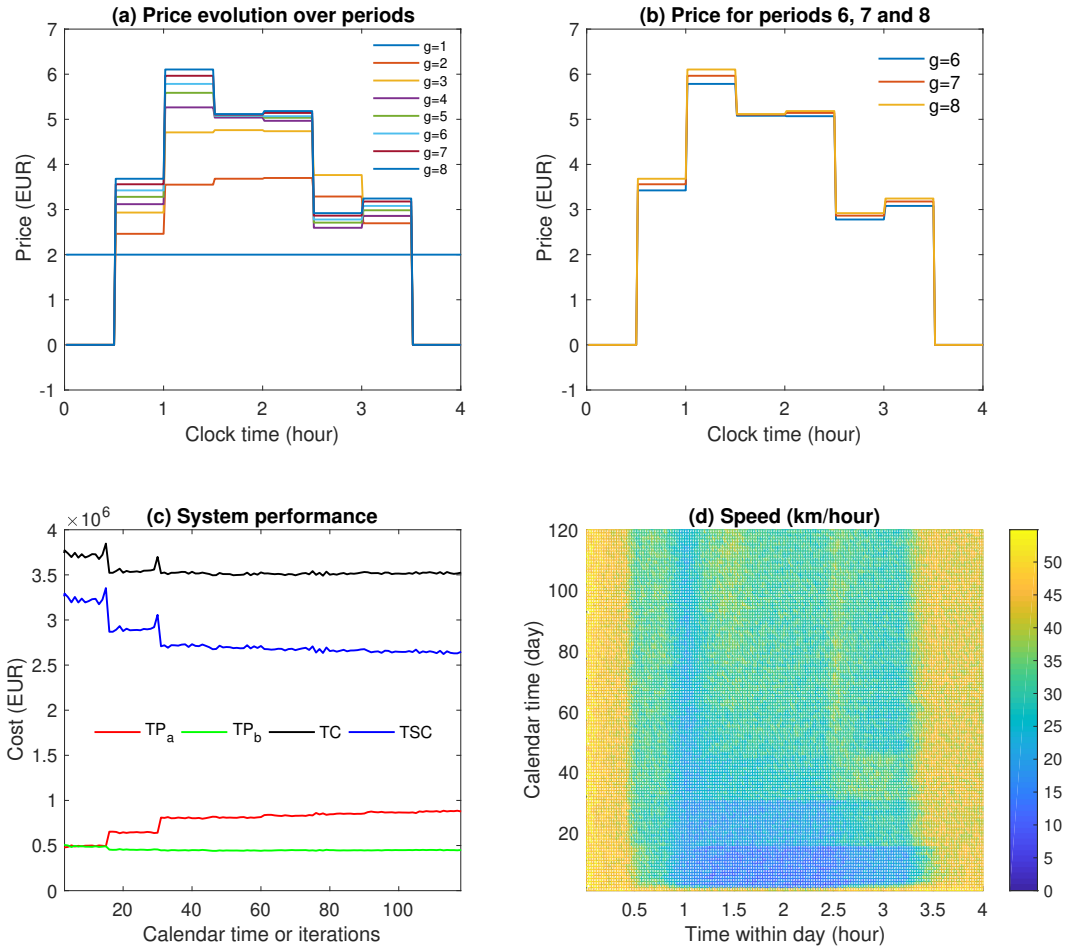

Figure 18: Evolution of pricing levels, system efficiency, and speed profile: the Northwestern speed model case

Figure 19 further shows the system performance under the period-to-period adaptive pricing levels after we varied the levels of uncertainty (i.e., $\pm 0\%$, $\pm 10\%$, $\pm 20\%$), which is similar to that illustrated by Figure 13 in Section 4.3. Similarly, we omit the results for the pricing levels and speed profile, which are very similar to those in Figure 18 (with minor differences). As can be seen from Figure 19, when the variations are different, the adaptive pricing scheme still leads to similar system performance (with slight difference under different levels of variations). In addition, larger variations in n_{cri} and v_{cri} lead to larger variations in TSC. These are consistent with observations from Figure 13.

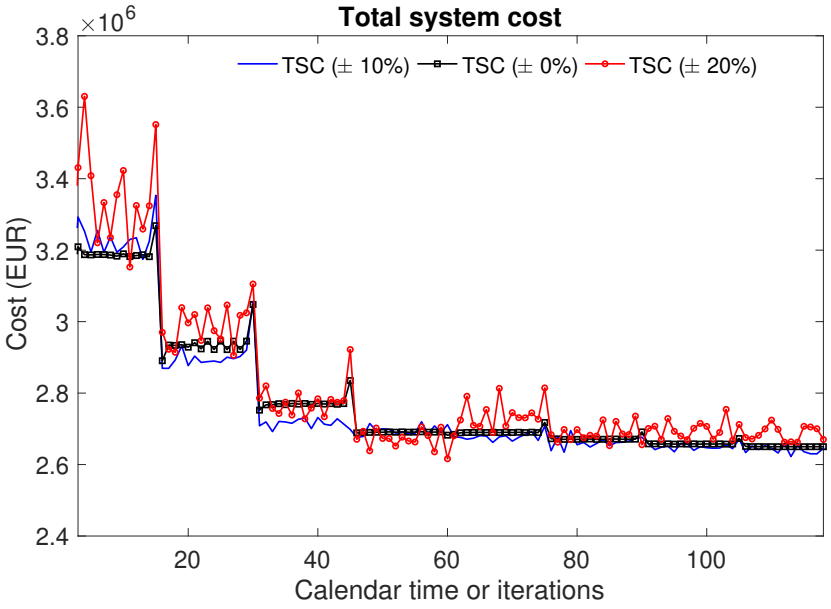

Figure 19: Evolution of total system costs given different levels of uncertainty: the Northwestern speed model case

References

Aghamohammadi, R. and Laval, J. A. (2018). Dynamic traffic assignment using the macroscopic fundamental diagram: A review of vehicular and pedestrian flow models. *Transportation Research Part B: Methodological*, in press.

Ambühl, L., Loder, A., Bliemer, M. C., Menendez, M., and Axhausen, K. W. (2018). A functional form with a physical meaning for the macroscopic fundamental diagram. *Transportation Research Part B: Methodological*, in press.

Amirgholy, M. and Gonzales, E. J. (2017). Efficient frontier of route choice for modeling the equilibrium under travel time variability with heterogeneous traveler preferences. *Economics of Transportation*, 11:1–14.

Amirgholy, M., Shahabi, M., and Gao, H. O. (2017). Optimal design of sustainable transit systems in congested urban networks: A macroscopic approach. *Transportation Research Part E: Logistics and Transportation Review*, 103:261–285.

Arnott, R. (2013). A bathtub model of downtown traffic congestion. *Journal of Urban Economics*, 76:110–121.

Arnott, R., De Palma, A., and Lindsey, R. (1990). Economics of a bottleneck. *Journal of Urban Economics*, 27(1):111–130.

Arnott, R., Kokoza, A., and Naji, M. (2016). Equilibrium traffic dynamics in a bathtub model: A special case. *Economics of Transportation*, 7:38–52.

Batista, S., Leclercq, L., and Geroliminis, N. (2019). Estimation of regional trip length distributions for the calibration of the aggregated network traffic models. *Transportation Research Part B: Methodological*, 122:192–217.

Ben-Akiva, M., Cyna, M., and De Palma, A. (1984). Dynamic model of peak period congestion. *Transportation Research Part B: Methodological*, 18(4-5):339–355.

Bie, J. and Lo, H. K. (2010). Stability and attraction domains of traffic equilibria in a day-to-day dynamical system formulation. *Transportation Research Part B: Methodological*, 44(1):90–107.

Bifulco, G. N., Cantarella, G. E., Simonelli, F., and Velonà, P. (2016). Advanced traveller information systems under recurrent traffic conditions: Network equilibrium and stability. *Transportation Research Part B: Methodological*, 92:73–87.

Cantarella, G. E. (2013). Day-to-day dynamic models for intelligent transportation systems design and appraisal. *Transportation Research Part C: Emerging Technologies*, 29:117–130.

Cantarella, G. E. and Cascetta, E. (1995). Dynamic processes and equilibrium in transportation networks: Towards a unifying theory. *Transportation Science*, 29(4):305–329.

Cantarella, G. E., Velonà, P., and Watling, D. P. (2015). Day-to-day dynamics and equilibrium stability in a two-mode transport system with responsive bus operator strategies. *Networks and Spatial Economics*, 15(3):485–506.

Cascetta, E. and Cantarella, G. E. (1991). A day-to-day and within-day dynamic stochastic assignment model. *Transportation Research Part A: General*, 25(5):277–291.

Chiabaut, N. (2015). Evaluation of a multimodal urban arterial: The passenger macroscopic fundamental diagram. *Transportation Research Part B: Methodological*, 81:410–420.

Chow, A. H. (2009). Properties of system optimal traffic assignment with departure time choice and its solution method. *Transportation Research Part B: Methodological*, 43(3):325–344.

Daganzo, C. F., Gayah, V. V., and Gonzales, E. J. (2011). Macroscopic relations of urban traffic variables: Bifurcations, multivaluedness and instability. *Transportation Research Part B: Methodological*, 45(1):278–288.

Dakic, I. and Menendez, M. (2018). On the use of lagrangian observations from public transport and probe vehicles to estimate car space-mean speeds in bi-modal urban networks. *Transportation Research Part C: Emerging Technologies*, 91:317–334.

Drake, J., Schofer, J., and May, A. (1965). A statistical analysis of speed-density hypotheses. *Traffic Flow and Transportation*.

Fosgerau, M. (2015). Congestion in the bathtub. *Economics of Transportation*, 4(4):241–255.

Friesz, T. L., Bernstein, D., Smith, T. E., Tobin, R. L., and Wie, B.-W. (1993). A variational inequality formulation of the dynamic network user equilibrium problem. *Operations Research*, 41(1):179–191.

Gayah, V. V. and Daganzo, C. F. (2011). Clockwise hysteresis loops in the macroscopic fundamental diagram: an effect of network instability. *Transportation Research Part B: Methodological*, 45(4):643–655.

Gayah, V. V., Gao, X. S., and Nagle, A. S. (2014). On the impacts of locally adaptive signal control on urban network stability and the macroscopic fundamental diagram. *Transportation Research Part B: Methodological*, 70:255–268.

Geroliminis, N. (2015). Cruising-for-parking in congested cities with an MFD representation. *Economics of Transportation*, 4(3):156–165.

Geroliminis, N. and Daganzo, C. F. (2008). Existence of urban-scale macroscopic fundamental diagrams: Some experimental findings. *Transportation Research Part B: Methodological*, 42(9):759–770.

Geroliminis, N. and Levinson, D. M. (2009). Cordon pricing consistent with the physics of overcrowding. In *Transportation and Traffic Theory 2009: Golden Jubilee*, pages 219–240. Springer.

Geroliminis, N. and Sun, J. (2011). Hysteresis phenomena of a macroscopic fundamental diagram in freeway networks. *Transportation Research Part A: Policy and Practice*, 45(9):966–979.

Geroliminis, N., Zheng, N., and Ampountolas, K. (2014). A three-dimensional macroscopic fundamental diagram for mixed bi-modal urban networks. *Transportation Research Part C: Emerging Technology*, 42:168–181.

Gonzales, E. J. (2015). Coordinated pricing for cars and transit in cities with hypercongestion. *Economics of Transportation*, 4(1-2):64–81.

Gonzales, E. J. and Daganzo, C. F. (2012). Morning commute with competing modes and distributed demand: User equilibrium, system optimum, and pricing. *Transportation Research Part B: Methodological*, 46(10):1519–1534.

Guo, R.-Y. and Huang, H.-J. (2016). A discrete dynamical system of formulating traffic assignment: Revisiting Smith's model. *Transportation Research Part C: Emerging Technologies*, 71:122–142.

Guo, R.-Y. and Szeto, W. (2018). Day-to-day modal choice with a Pareto improvement or zero-sum revenue scheme. *Transportation Research Part B: Methodological*, 110(1):1–25.

Guo, R.-Y., Yang, H., and Huang, H.-J. (2018). Are we really solving the dynamic traffic equilibrium problem with a departure time choice? *Transportation Science*, 52(3):603–620.

Haddad, J. and Zheng, Z. (2018). Adaptive perimeter control for multi-region accumulation-based models with state delays. *Transportation Research Part B: Methodological*, in press.

Herrera, J. C., Work, D. B., Herring, R., Ban, X. J., Jacobson, Q., and Bayen, A. M. (2010). Evaluation of traffic data obtained via GPS-enabled mobile phones: The Mobile Century field experiment. *Transportation Research Part C: Emerging Technologies*, 18(4):568–583.

Hofleitner, A., Herring, R., Abbeel, P., and Bayen, A. (2012). Learning the dynamics of arterial traffic from probe data using a dynamic Bayesian network. *IEEE Transactions on Intelligent Transportation Systems*, 13(4):1679–1693.

Iryo, T. (2008). An analysis of instability in a departure time choice problem. *Journal of Advanced Transportation*, 42(3):333–358.

Iryo, T. (2016). Day-to-day dynamical model incorporating an explicit description of individuals' information collection behaviour. *Transportation Research Part B: Methodological*, 92:88–103.

Kouvelas, A., Saeedmanesh, M., and Geroliminis, N. (2017). Enhancing model-based feedback perimeter control with data-driven online adaptive optimization. *Transportation Research Part B: Methodological*, 96:26–45.

Lamotte, R. and Geroliminis, N. (2018). The morning commute in urban areas with heterogeneous trip lengths. *Transportation Research Part B: Methodological*, 117:794–810.

Leclercq, L. and Geroliminis, N. (2013). Estimating MFDs in simple networks with route choice. *Transportation Research Part B: Methodological*, 57:468–484.

Leclercq, L., Sénécat, A., and Mariotte, G. (2017). Dynamic macroscopic simulation of on-street parking search: A trip-based approach. *Transportation Research Part B: Methodological*, 101:268–282.

Lehe, L. J. (2017). Downtown tolls and the distribution of trip lengths. *Economics of Transportation*, 11:23–32.

Li, X., Liu, W., and Yang, H. (2018). Traffic dynamics in a bi-modal transportation network with

information provision and adaptive transit services. *Transportation Research Part C: Emerging Technologies*, 91:77–89.

Li, X. and Yang, H. (2016). Dynamics of modal choice of heterogeneous travelers with responsive transit services. *Transportation Research Part C: Emerging Technologies*, 68:333–349.

Lindsey, R. (2004). Existence, uniqueness, and trip cost function properties of user equilibrium in the bottleneck model with multiple user classes. *Transportation Science*, 38(3):293–314.

Liu, W. (2018). An equilibrium analysis of commuter parking in the era of autonomous vehicles. *Transportation Research Part C: Emerging Technologies*, 92:191–207.

Liu, W. and Geroliminis, N. (2016). Modeling the morning commute for urban networks with cruising-for-parking: An MFD approach. *Transportation Research Part B: Methodological*, 93:470–494.

Liu, W. and Geroliminis, N. (2017). Doubly dynamics for multi-modal networks with park-and-ride and adaptive pricing. *Transportation Research Part B: Methodological*, 102:162–179.

Liu, W., Li, X., Zhang, F., and Yang, H. (2017). Interactive travel choices and traffic forecast in a doubly dynamical system with user inertia and information provision. *Transportation Research Part C: Emerging Technologies*, 85:711–731.

Liu, W., Yang, H., Yin, Y., and Zhang, F. (2014). A novel permit scheme for managing parking competition and bottleneck congestion. *Transportation Research Part C: Emerging Technologies*, 44:265–281.

Lo, H. K. and Szeto, W. Y. (2002). A cell-based variational inequality formulation of the dynamic user optimal assignment problem. *Transportation Research Part B: Methodological*, 36(5):421–443.

Loder, A., Ambühl, L., Menendez, M., and Axhausen, K. W. (2017). Empirics of multi-modal traffic networks–Using the 3D macroscopic fundamental diagram. *Transportation Research Part C: Emerging Technologies*, 82:88–101.

Long, J., Szeto, W., Huang, H.-J., and Gao, Z. (2015). An intersection-movement-based stochastic dynamic user optimal route choice model for assessing network performance. *Transportation Research Part B: Methodological*, 74:182–217.

Mahmassani, H. S. and Liu, Y.-H. (1999). Dynamics of commuting decision behaviour under advanced traveller information systems. *Transportation Research Part C: Emerging Technologies*, 7(2):91–107.

Mariotte, G., Leclercq, L., and Laval, J. A. (2017). Macroscopic urban dynamics: Analytical and numerical comparisons of existing models. *Transportation Research Part B: Methodological*, 101:245–267.

Mazloumian, A., Geroliminis, N., and Helbing, D. (2010). The spatial variability of vehicle densities as determinant of urban network capacity. *Philosophical Transactions of the Royal Society of London A: Mathematical, Physical and Engineering Sciences*, 368(1928):4627–4647.

Nadaraya, E. A. (1964). On estimating regression. *Theory of Probability & Its Applications*, 9(1):141–142.

Ramezani, M., Haddad, J., and Geroliminis, N. (2015). Dynamics of heterogeneity in urban networks: Aggregated traffic modeling and hierarchical control. *Transportation Research Part B: Methodological*, 74:1–19.

Saberi, M. and Mahmassani, H. S. (2012). Exploring properties of networkwide flow–density rela-

tions in a freeway network. *Transportation Research Record*, 2315(1):153–163.

Saeedmanesh, M. and Geroliminis, N. (2016). Clustering of heterogeneous networks with directional flows based on "Snake" similarities. *Transportation Research Part B: Methodological*, 91:250–269.

Smith, M. J. (1984). The stability of a dynamic model of traffic assignment–An application of a method of Lyapunov. *Transportation Science*, 18(3):245–252.

Smith, M. J. and Watling, D. P. (2016). A route-swapping dynamical system and Lyapunov function for stochastic user equilibrium. *Transportation Research Part B: Methodological*, 85:132–141.

Vickrey, W. S. (1969). Congestion theory and transport investment. *The American Economic Review*, pages 251–260.

Wardrop, J. G. (1952). Some theoretical aspects of road traffic research. *Proceedings of the Institution of Civil Engineers*, 1(3):325–362.

Watling, D. (1999). Stability of the stochastic equilibrium assignment problem: A dynamical systems approach. *Transportation Research Part B: Methodological*, 33(4):281–312.

Watson, G. S. (1964). Smooth regression analysis. *Sankhyā: The Indian Journal of Statistics, Series A*, pages 359–372.

Xiao, Y. and Lo, H. K. (2016). Day-to-day departure time modeling under social network influence. *Transportation Research Part B: Methodological*, 92:54–72.

Yang, H., Liu, W., Wang, X., and Zhang, X. (2013). On the morning commute problem with bottleneck congestion and parking space constraints. *Transportation Research Part B: Methodological*, 58:106–118.

Yildirimoglu, M. and Geroliminis, N. (2013). Experienced travel time prediction for congested freeways. *Transportation Research Part B: Methodological*, 53:45–63.

Yildirimoglu, M. and Geroliminis, N. (2014). Approximating dynamic equilibrium conditions with macroscopic fundamental diagrams. *Transportation Research Part B: Methodological*, 70:186–200.

Yildirimoglu, M. and Ramezani, M. (2019). Demand management with limited cooperation among travellers: A doubly dynamic approach. *Transportation Research Part B: Methodological*, in press.

Zhang, F., Lindsey, R., and Yang, H. (2016). The Downs–Thomson paradox with imperfect mode substitutes and alternative transit administration regimes. *Transportation Research Part B: Methodological*, 86:104–127.

Zhang, F., Liu, W., Wang, X., and Yang, H. (2017). A new look at the morning commute with household shared-ride: How does school location play a role? *Transportation Research Part E: Logistics and Transportation Review*, 103:198–217.

Zhang, F., Yang, H., and Liu, W. (2014). The Downs–Thomson Paradox with responsive transit service. *Transportation Research Part A: Policy and Practice*, 70:244–263.

Zhang, F., Zheng, N., Yang, H., and Geroliminis, N. (2018). A systematic analysis of multimodal transport systems with road space distribution and responsive bus service. *Transportation Research Part C: Emerging Technologies*, 96:208–230.